Design of a Size Reduced Antenna Array for Angle of Arrival (AoA) Estimation for BLE 5.1

FELIX LÅNGBERG & JONAS THURBORG
DEPARTMENT OF ELECTRICAL AND INFORMATION TECHNOLOGY
FACULTY OF ENGINEERING | LTH | LUND UNIVERSITY

Design of a Size Reduced Antenna Array for Angle of Arrival (AoA) Estimation for BLE 5.1

Felix Långberg & Jonas Thurborg
elt15fla@student.lu.se & elt15jth@student.lu.se

Department of Electrical and Information Technology
Lund University

Supervisor: Daniel Sjöberg

Company supervisors: Olof Viklund & Aneeb Sohail

Examiner: Mats Gustafsson

September 4, 2020

Printed in Sweden
Tryckeriet i E-huset, Lund

Abstract

Bluetooth low energy (BLE) 5.1 allows for Angle of Arrival(AoA) measurements which in turn requires antenna arrays to be used. These arrays must be low power which results in that an efficient switching pattern is applied and for greater field of view good omnidirectivity is necessary. BLE devices are typically small in size and therefore size reduction of these arrays are of interest. The typical spacing between antennas in arrays are 0.5λ which is around 6 cm and become rather large. In this thesis a size reduced L-shaped antenna array consisting of three antenna elements with 0.3λ spacing is simulated. Two major studies were made with various spacings between 0.25 and 0.5λ, both physical measurements on a three element prototype array and simulations showed that 0.3λ was the smallest spacing achievable without compromising AoA compatibility. The final simulated antenna array shows peak gain at 2.55 dB and resonance at 2.44 GHz as well as a field of view of around 100 degrees.

Popular Science Summary

The usage of device detection is something that has been around since the 1930s. The development of RAdio Detection And Ranging (RADAR)[1] is what laid the ground for today's way of detecting devices. The basic principle of radar detection is that an electromagnetic wave transmitted by an antenna is reflected at objects and is subsequently received by the same, or a different, antenna. From the received signal the radar can then calculate the delay between the outgoing and the incoming wave, and thus calculate a distance to the object. In addition radars are also capable of detecting the direction to the discovered object, this is made possible by the use of beam steering. This is done by having multiple antennas as transceivers and weighted in such a way that their radiation pattern interfere with one another to form a common beam, known as a phased array. The weights of the antennas are then altered in such a fashion that the common beam sweeps a span of interest of detection.

The recent releases in Bluetooth (BLE 5.1) have made it possible to detect other Bluetooth devices in the vicinity and the direction they are in. This is called measuring the Angle of Arrival(AoA) or Direction of Arrival (DoA). BLE devices are subject to very restricted power consumption which limits the amount of antennas that can be active at a point in time. This results in that beam steering is impossible for BLE devices. How this is solved can be seen as beam steering in reverse, namely having a switched antenna array that receives the signal and measures the phase difference between the antennas of the incoming wave. Knowing the phase difference of the antennas is practically the same as knowing the weights of antennas in an array that is able to implement beam steering.

In a phased array the spacing of the antennas is of great importance. Traditional arrays have the spacing of half the wavelength of the frequency for which the array is meant to operate at. This is in order to use as few elements as possible and still be able to scan arbitrary angles without grating lobes. As mentioned BLE 5.1 allows devices to implement AoA and these devices tend to be compact with a smart design raising the question if AoA is implementable with antenna arrays where the spacing is smaller than half a wavelength. This thesis will try try to find the consequences of making the arrays more compact and how well a minimized system can perform.

Acknowledgements

We would like to express our greatest gratitude to all persons who have been a part of the process during this master thesis:

Our supervisor at LTH, Professor Daniel Sjöberg at the Faculty of Engineering at LTH, for his guidance and great comments on our work through the entire process.

Our supervisors at u-blox, Olof Viklund and Aneeb Sohail, for their encouragement and will to be there as mentors for our first project outside the academic world. They have brought forth valuable comments and insights on how a product is developed and have aided us throughout the entire process.

Brian Curran, for his great inputs in both simulation and results, he has been a great part in the simulation of the design which we are grateful for.

Andreas Karlqvist, for his help implementing algorithms and providing helpful knowledge.

Finally we would like to express a huge thank you to the entire team at u-blox Malmö for believing in us and making our stay very enjoyable. Thank you!

Lund, September 4, 2020
Felix Långberg & Jonas Thurborg

Table of Contents

List of Figures

List of Tables

List of Acronyms

AoA Angle of Arrival

DoA Direction of Arrival

BLE Bluetooth low energy

RF Radio Frequency

IF Intermediate Frequency

PCB Printed Circuit Board

MUSIC MUltiple SIgnal Classification

CTE Continious Tone Extenstion

SNR Signal to Noise Ratio

Chapter 1
Introduction

1.1 Background and the Company

This thesis is done in collaboration with u-blox Malmö. u-blox has a short range (including; Bluetooth Wi-Fi) team stationed in Malmö, that has since the release of BLE 5.1 been working on different software and hardware aspects of AoA. The published master thesis for a reduced size antenna array for AoA applications, will be a part of their catalog for customers who are interested in indoor positions for various applications. To be at the forefront of Bluetooth low energy devices in the consumer market, it is desirable to be able to offer a compact, smart, low energy and effective Bluetooth module with AoA capability.

1.2 Thesis Goal

The goal is to minimize the size of and simulate an antenna array applicable for BLE 5.1 and implementable for AoA. The array should measure an accuracy in angle of arrival at an acceptable error of 10 degrees at around 5 meter distance. The array was chosen to be not larger than 3 antennas in each dimension and be printed on a PCB with a specific layer structure.

1.3 Thesis Work Division

The work has been divided between the authors as evenly as possible. Background information has been collected by both students as well as the physical measurements on the array. The simulations have been done by both students as well but in order to optimize time consumption Jonas has done most of the HFSS simulations that led to a desired result while Felix has done most of the Matlab simulations. The Matlab script used was designed by both students working together to develop an as good as possible MUSIC algorithm for the physical measurements as well as the synthetic data simulations. The simulations in HFSS were also performed by both students while most of the work resulting in the finished antenna array PCB design was designed mainly by Jonas while still being a collaboration by both students. The report has been worked on simultaneously by both students.

1.4 Outline

This report starts with antenna theory. Here is presented different antenna characteristics such as radiation pattern, bandwidth, patch antennas and different antenna tuning methods Following this, theory regarding AoA is summarized. The MUSIC algorithm is introduced and explained. From there the different hardware and software tools used in the simulations are explained as well as physical measurements. This leads into the method chapter, where various simulations and tests are summarized and explained, as well as how they performed and how the results are acquired.

Following the method chapter there are two chapters where the various results are presented, with respect to both measurements and simulations. The simulations produced a lot of data so an explanation in how the result tables are interpreted is given in this chapter as well as the results of interest. The majority of the tables are found in the Appendix A. Following these chapters are the discussions and conclusions followed by future work where there is discussed how different measures can be taken to improve the results presented in this thesis.

1.5 Delimitations

There are a couple of delimitations put onto this thesis work. Without all of these delimitations an optimal spacing for size reduction and still being able to measure AoA would simply depend on too many variables such as gain, radiation patterns, transmission distance and so on. The main delimitation is the use of only patch antennas in simulations. The second delimitation was to only use one set of software in order to compute AoA as well as only one version of a MUSIC algorithm. All frequencies used are in the bluetooth spectrum. Only linearly polarized antenna elements were considered. 16 IQ samples were gathered per half wavelength of the modulated signal by BLE 5.1 when used for AoA measurements. Which results in a angle resolution of $\frac{180}{16} = 12$ degrees. The final delimitation was having the antenna elements seperated, i.e not overlapping, which means that the antenna element size sets the lower limit of possible spacings to test. Measurements on the physical array were not achievable due to manufacturing delay as well as missing software.

Chapter 2
Antenna Theory

2.1 Frequency Bands

In wireless communication signals can be transmitted over various frequency bands. The radio frequency spectrum is divided into different sub frequency bands as seen in Table 2.1 where different bands are used for different communication scenarios [4].

Band	Frequency	Wavelength
VLF	3 kHz - 30 kHz	100 km - 10 km
LF	30 kHz - 300 kHz	10 km - 1 km
MF	300 kHz - 3 MHz	1 km - 100 m
HF	3 MHz - 30MHz	100 m - 10 m
VHF	30 MHz- 300 MHz	10 m - 1 m
UHF	300 MHz - 3 GHz	1 m - 100 mm
SHF	3 GHz - 30GHz	100 mm - 10 mm
EHF	30 GHz - 300 GHz	10 mm - 1 mm

Table 2.1: Wireless communication frequency bands.

2.1.1 BLE 5.1

Bluetooth is a standard that is used for data transmission for short range communication between devices. Bluetooth operates in the UHF band and uses the 2.4 GHz ISM spectrum band 2.400 - 2.483.5 GHz. BLE or Bluetooth Low Energy is designed for low power consumption. To enable reliable operation in the
2.4 GHz band it transmits data over 79 channels using frequency hopping spread spectrum approach [5].

$$\text{Bluetooth frequency channels (MHz)} = 2402 + k, k = 0, 1, ..., 78 \tag{2.1}$$

BLE 5.1 offers direction finding features and is capable of pinpointing physical locations of devices, which aids in indoor positioning. Since BLE is designed for

low power consumption it limits the number of active antenna elements at a certain instant [6]. This forces the position detection devices to implement some sort of antenna switching scheme in order to lower the power consumption. Compare this with a switched beam system used in [?] for AoA measurements where there are multiple antennas scanning the surroundings for the highest received power. The step up from BLE 5.0 is that devices are now not only able to use signal strength to determine distance but now also use signal phase to find the direction of the device in its proximity. The use cases are proposed as finding your keys and to enable smarthome hardware to pinpoint your location for faster and energy efficient data transfer.

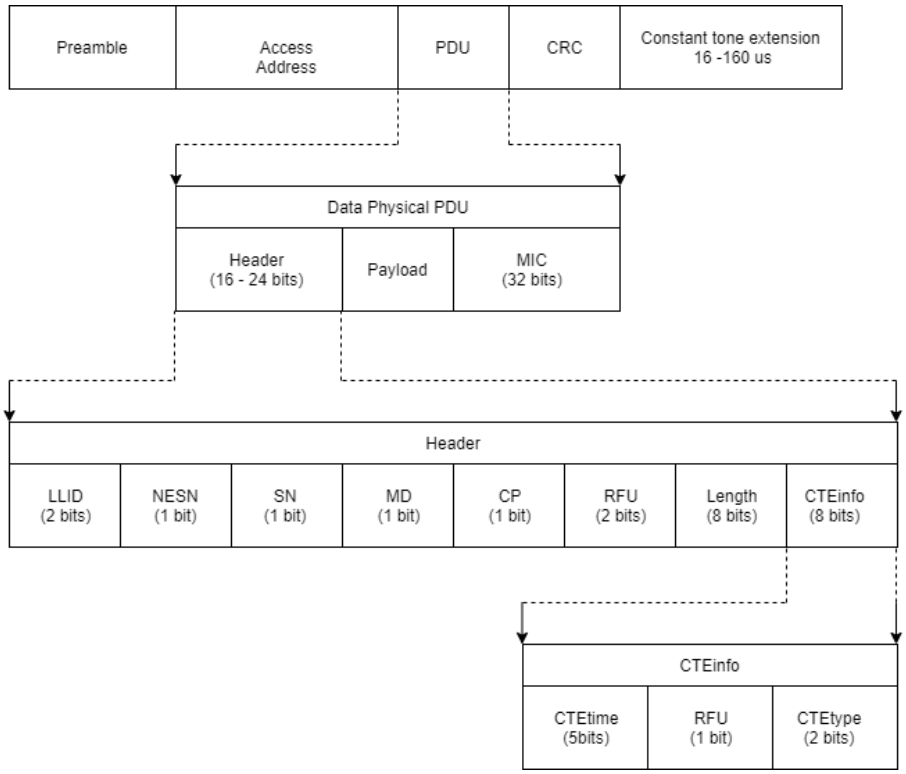

Figure 2.1: BLE 5.1 Packet format.

The signals used to gather AoA information are based on CTE (continuous tone extension) [7] which in our case is a pure tone of 250Khz + the current channel frequency [8]. The reason for this is due to not wanting to have phase modulation during the already precise phase measurements required for AoA. However the usual bluetooth protocols still need to be used and addressed to start the transmission [7] an example of this is shown in Figure 2.1. During the packet formatting no switching should occur as this might cause issues during the setup of the transmission.

To prove that the the 250 kHz tone that the IQ data is measured from inherits the phase difference of the RF signal can be done by using the formula

$$\cos(\alpha) \cdot \cos(\beta) = \frac{1}{2}(\cos(\alpha + \beta) + \cos(\alpha - \beta)) \tag{2.2}$$

where $\alpha = (f_1 + f_2)2\pi + \theta$ and $\beta = 2\pi f_1$. Using these the left side of Equation 2.2 becomes

$$\cos((f_1 + f_2)2\pi + \theta) \cdot \cos(2\pi f_1) \tag{2.3}$$

which in turn can be re written into.

$$\frac{1}{2}(\cos(((2f_1 + f_2)2\pi + \theta)) + \cos(2\pi f_2 + \theta) \tag{2.4}$$

If f_1 is an RF frequency and f_2 an IF frequency then with the use of a low pass filter that only lets frequencies close to f_2 pass, the cos signal with the RF frequency will be filtered out and only the IF signal is left. Note that the cos signal with the IF frequency inherited the phase difference θ [8].

2.2 Antenna Radiation

2.2.1 Near-field and far-field

The radiated field emanating from an antenna element can be divided into three regions. The first one surrounds the antenna element, called the reactive near-field. The second one is far away from the antenna element, called the far-field or the Fraunhofer field. The third one is called the radiating near field (Fresnel region) and is located in between the near and far-field. All of the regions are shown in Figure 2.2. The far-field is the most important one as antennas are mostly used in the far-field. The wave propagation is considered a plane wave in the far field and does not change with increasing distance from the point source [2] which is ideal in phase-measurements. The distances required to be in each of the fields are given by Equations (2.5) and (2.6).

$$r_2 > \frac{2D^2}{\lambda} \tag{2.5}$$

$$r_1 > 0.62\sqrt{\frac{D^3}{\lambda}} \tag{2.6}$$

The reactive near field is a region that is mainly occupied with a reactive field where the electric (E) and the magnetic (H) fields are 90 degrees out of phase of each other, hence the name reactive.

The radiating near field is occupied with radiated field much like the far field but the wave propagation is still dependent on the distance from the source. In this region measurements of E and H should be done separately and the source should not be approximated as a point source which is the case in far-field [9].

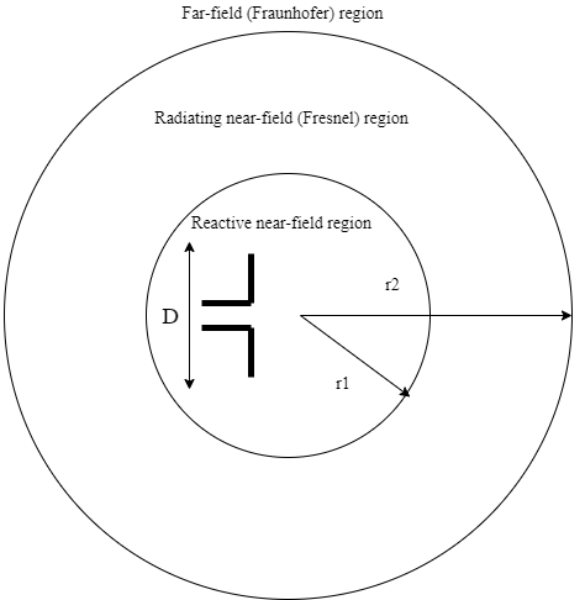

Figure 2.2: Show the relation between distance and field regions. Based on Figure 2.7 from [2].

2.2.2 Radiation pattern

The radiation pattern of an antenna is a representation of the radiation in the far field. Different antenna element have different radiation pattern dependent on the current waves traveling along the antenna. The radiation property most often displayed as a radiation pattern is radiated energy as a function of the receivers position along a surface of a constant radius [2].

There are three basic different radiation pattern types, isotropic, directional and omnidirectional. Isotropic radiation patterns radiate uniformly in all directions horizontal and vertically alike from a point source which can only be utilized in theory and can not be produced in a real world scenario. It is used as a reference to compare other radiation patterns. The directional radiation pattern focuses the radiation intensity in a certain direction which makes it radiate less towards the other directions. Omnidirectional antennas radiate equally in a certain plane, for example the horizontal plane. In this plane the radiation intensity is equal in all azimuth angles whilst loosing intensity with an increasing vertical angle.

These radiation patterns are commonly shown in a 3D-plot like Figure 2.3. The figure also shows how a radiation pattern can be represented in 2 dimensions, but to get the full information of the radiation pattern three 2D plots are needed. This specific radiation pattern radiates most of its energy in the horizontal plane (XY-plane) but almost nothing along the Z axis.

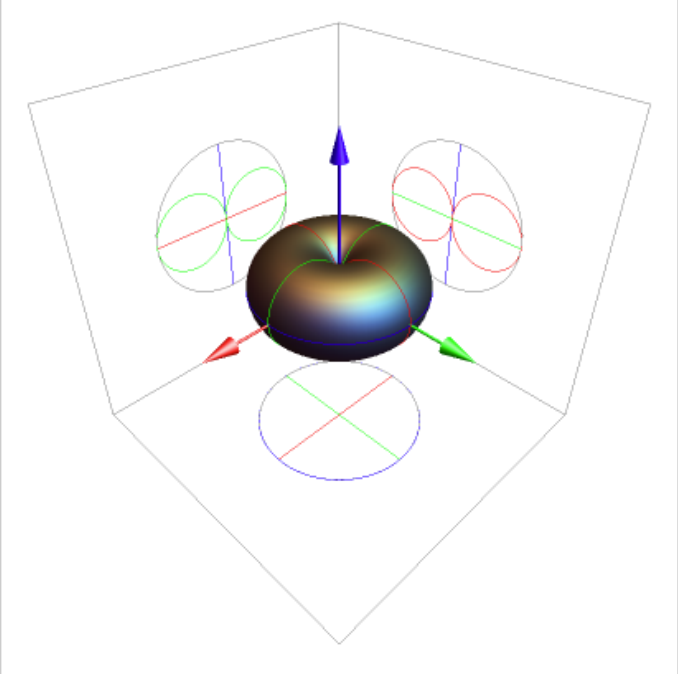

Figure 2.3: 3D radiation pattern showing all three 2D pattern [3].

2.2.3 Directivity

An antenna's directivity is a measure of how much of the radiated energy is in a certain direction compared to an isotropic antenna (which radiates equally everywhere) with the same amount of radiated energy. The directive antenna will radiate more energy in a certain direction and therefore achieve a higher directivity but as it has a high directivity in a certain direction it also has lower directivity in the other directions, as the sum of all the radiated energy is the same between the directed antenna and the isotropic one. The expression explaining this is shown in Equation (2.7). It is a measure of the ability to radiate its energy in a certain direction.

$$D(\theta,\phi) = \frac{4\pi U(\theta,\phi)}{P_t} = \frac{4\pi U(\theta,\phi)}{\iint U d\Omega} \tag{2.7}$$

Assume that the maximum directivity is in the direction (θ_0, ϕ_0) then maximum directivity $D_{\max}$ is

$$D_{\max} = \frac{4\pi U_{\max}}{\iint U d\Omega} \tag{2.8}$$

where $U_{\max}$ is the radiation intensity in the direction where U has its highest value $U(\theta_0, \phi_0)$ [10].

2.2.4 The Friis transmission formula

The Friis formula gives the received power of your antenna element.

$$P_r = \frac{P_t G_t G_r \lambda^2}{(4\pi R)^2} \tag{2.9}$$

The formula depends on the gains of the transmitting and receiving antennas G_t and G_r, the wavelength λ, the distance between them R and the transmitted power P_t. It can used as an estimator for the anticipated received power in your antenna element which is crucial when designing wireless systems [2].

2.2.5 Polarization

The polarization of a plane wave is defined to be the direction of the electrical field (note that this direction is not the propagation direction). For example the electric field in Equation 2.10 has polarization in the x-direction

$$\boldsymbol{E}(z,t) = \hat{\boldsymbol{x}} A \mathrm{e}^{\mathrm{j}(\omega t - kz)} \tag{2.10}$$

where the propagation direction is in the $\hat{\boldsymbol{z}}$ direction, t is time, A is the amplitude of the wave, $k = \frac{2\pi}{\lambda}$, and ω is the angular frequency. There are three possible polarizations, linear, elliptical and circular. These are obtained from a phase shift between the x and y component of the electrical field. The radiated fields depend on the current waves of the antenna, these in turn give rise to a radiated electrical field which polarization is dependent on the direction of the current wave. If the physical orientation of the antenna were to be tilted in space so would the polarization of the electrical field as it inherits the direction from the current waves of the antenna. This in turn raises an issue where two identical antennas might not be able to communicate well with each other if one of them is tilted 90 degrees (from x polarization to y polarization) as the electric field incident on the receiving antenna can not excite the same current waves that the original antenna transmitted. The polarization loss factor is a measure of how much power is lost due to polarization mismatch between two antenna elements

$$\mathrm{PLF} = \cos^2 \phi \tag{2.11}$$

where ϕ is the angular difference between the two linear polarized antennas. Table 2.2 shows the amount of losses of a couple common scenarios.

Transmit polarization	Receive polarization	Theoretical loss
Vertical	Vertical	0dB
Vertical	Slant (45 or 135)	-3dB
Vertical	Horizontal	$-\infty$
Vertical	Circular (RHCP or LHCP)	-3dB
Horizontal	Horizontal	0dB
Horizontal	Slant (45 or 135)	-3dB
Horizontal	Circular (RHCP or LHCP)	-3dB
Circular (RHCP)	Circular (RHCP)	0dB
Circular (RHCP)	Circular (LHCP)	$-\infty$
Circular (RHCP or LHCP)	Slant (45 or 135)	-3dB

Table 2.2: Polarization mismatch loss.

2.3 Antenna characteristics

2.3.1 Radiation resistance

The current distribution on an antenna element is related to its length. Different frequencies distribute different currents on a fixed length antenna due to the fact that the wavelengths differ. Assume then a constant frequency and therefore a constant wavelength, this frequency will give rise to different current distributions on antennas with different lengths as seen in Figure 2.4 [2].

Since the current distribution is different across the antenna element depending on where you measure it, what is called the radiation resistance will differ accordingly. The radiation resistance for a $\lambda/2$ dipole is 73Ω in free space when the feed point is in the middle of the dipole [2], as seen in Figure 2.4.

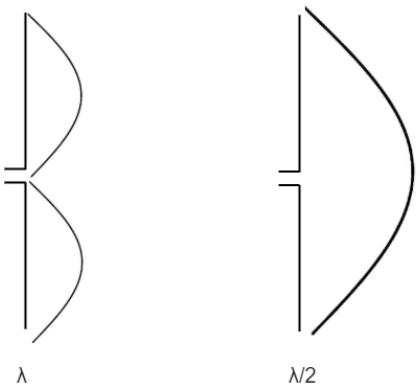

Figure 2.4: Current distribution on a dipole antenna for different lengths, λ and $\lambda/2$

2.3.2 Reflection coefficient

The reflection coefficient is an expression of how much power gets reflected back in the transmissions between two different ohmic environments [11]. The formula for the reflection coefficient is $\Gamma = \frac{Z_L - Z_0}{Z_L + Z_0}$ or the dB version in Equation (2.12).

$$\Gamma_{dB} = 10\log(\frac{Z_L - Z_0}{Z_L + Z_0}) \tag{2.12}$$

A scenario where $Z_L = Z_0$ results in a reflection coefficient of 0 which means that the total reflected power is 0 which in turn means that there are no losses due to reflection. The most common Z_0 is 50 Ω which means that the goal of most designs is to have the radiation resistance at 50Ω at the transmission frequency in order to avoid unnecessary losses. Coming back to what was mentioned in the previous part where the feed point was placed at the middle of the antenna element which meant that the radiation resistance was equal to 73 Ω. Putting in 73 Ω in the reflection coefficient formula for $Z_0 = 50\Omega$ gives a reflection coefficient of 0.18 which implies that some of the power is reflected back. Ideally the reflection coefficient should be as close to 0 as possible, to achieve this a matching network can be used.

2.3.3 Bandwidth

The bandwidth is the width in the frequency spectrum where the antenna is able to pick up signals, even though the antenna element is designed for a certain frequency small deviations from the frequency are still able to be received with a good signal strength. A larger frequency deviation results in an altered radiation resistance which in turn results in an altered reflection coefficient which causes losses. How much losses the system is specified to handle defines how wide the bandwidth can be. Figure 2.5 shows the bandwidth of an antenna element where the specification is that the S11 parameter is smaller than −10 dB, in this case the bandwidth is 28 MHz wide, which is sufficient when working in for example bluetooth.

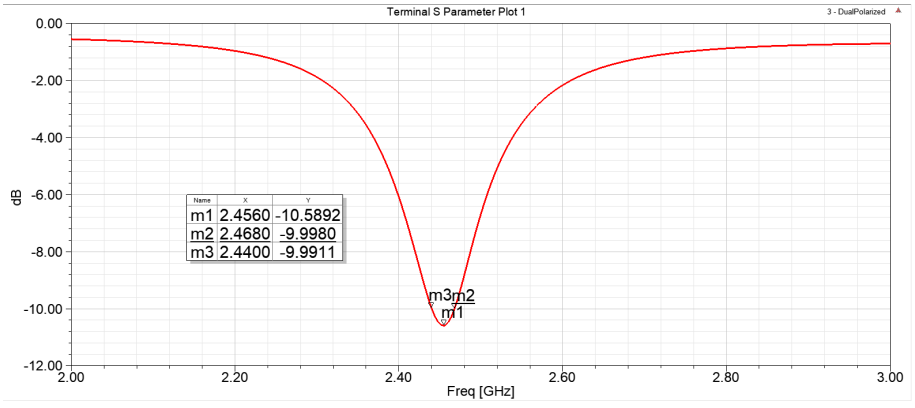

Figure 2.5: Bandwidth of an antenna element at Bluetooth frequencies.

2.3.4 Patch antenna

A patch antenna is a low cost, low profile easily fabricated antenna. The antenna is often fabricated directly on a circuit board and is made from a highly conductive material often copper [12] with the width and length of half a wavelength. The patch sits on top of a substrate with a certain permittivity. A patch antenna radiates due to fringing fields, the antenna can be seen as open circuited at its edges and that implies that there is no current at the edges while maximum current at the center due to it being half a wavelength in size. Since its edges can be seen as open circuit the reflection coefficient will be 1 here this will drive the current and voltage to be out of phase. This in turn will result in that the voltages at the opposite edges will be at maximum +V Volts and minimum -V Volts.

The parameters used when designing a patch antenna are its width, length, type of substrate, thickness of the substrate and feed position where all of these depend on the specifications on both frequency and bandwidth. The design flow starts with choosing a frequency the antenna should resonate at and then choosing a substrate. Then a width can be chosen as

$$W = \frac{c}{2f_r}\sqrt{\frac{2}{\varepsilon_r + 1}} \tag{2.13}$$

where c is the speed of light $3 \cdot 10^8$, ϵ_r is the dielectric constant of the chosen substrate and f_r is the desired frequency. The effective dielectric constant can be calculated as.

$$\varepsilon_{eff} = \frac{\varepsilon_r + 1}{2} + \frac{\varepsilon_r - 1}{2}\left(\frac{1}{\sqrt{1+\frac{2h}{W}}}\right) \tag{2.14}$$

The effective length can be calculated with as

$$L_{eff} = \frac{C}{2f_r\sqrt{\varepsilon_{eff}}} \tag{2.15}$$

The extension length can be calculated as

$$\Delta L = h \cdot 0.412 \cdot \frac{(\varepsilon_{eff} + 0.3)\left(\frac{W}{h} + 0.264\right)}{(\varepsilon_{eff} - 0.258)\left(\frac{W}{h} + 0.8\right)} \tag{2.16}$$

where h is the thickness of the substrate. Lastly the final L can be calculated as

$$L = L_{eff} - 2\Delta L \tag{2.17}$$

With all of these parameters the most basic patch antenna can be made to resonate at the desired frequency however its bandwidth may not be sufficient [13]. Note that a small change of these parameters create a sort of chain reaction where the resonance frequency might change. However this could also be used to an advantage when designing an antenna for a certain system.

Another important parameter for patch antennas is the feed position, as previously mentioned in Section 2.3.1. As the position of the feed point change how the antenna behaves, how well it still resonates at the desired frequency as well as the width of the bandwidth.

2.4 Antenna tuning

Antenna performance in theory will always differ from the theoretical values as there are many more impairing effects such as humans nearby or small amount of space at play in the real world [14]. Simulation software introduces some of these impairing effects and is a better tool to use than just formulas when designing antennas as the software tools introduces effects like mutual coupling between antenna elements, size of ground plane etc. One will quickly realise that even in the simulation software the antenna does not behave as well as it should according to the formulas and some tuning of the parameters will be needed. In the previous section the antenna parameters were gathered and all of these are viable parameters to tune. Note that some specifications require the antenna to be at a certain size or vice versa but that is up to the engineer at hand to work around. For example if the resonance turned out to be at a different value than desired an increase or decrease of the antenna element could result in the correct resonance.

2.4.1 The Smith chart

The Smith chart is a tool used by RF engineers for designing matching networks but it is far more diverse than that, in Figure 2.6 a Smith chart is depicted. For the sake of this thesis the Smith chart has mainly been used to design matching networks and this theory part will mainly explain that use case.

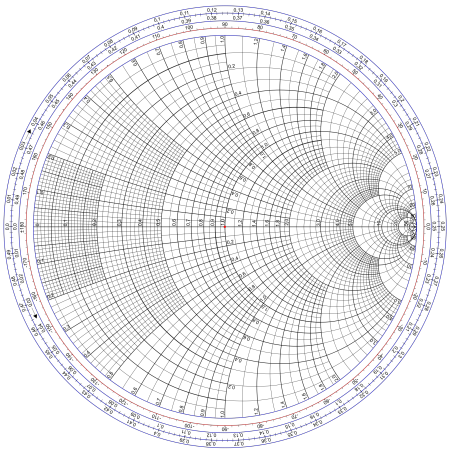

Figure 2.6: A depiction of the Smith chart.

The Smith chart is constructed based on the reflection coefficient Γ of a transmission line. It is a parameterized plot in polar coordinates of the general reflection coefficient within a circle of unit radius $|\Gamma| \leq 1$, where Γ is given by

$$\Gamma = \frac{Z_L - Z_0}{Z_l + Z_0} \tag{2.18}$$

where Z_L is the load impedance and Z_0 is the characteristic impedance of the transmission line of interest [15]. Instead of having a Smith chart for transmission lines of different characteristics impedances the impedances are all normalized to the characteristic impedance Z_0 of the transmission being used. The normalized impedance of interest is given by $z_L = \frac{Z_L}{Z_0} = r + jx$ where r and x are the real and imaginary parts of the normalized impedance, respectively. In the Smith chart the normalized resistance is to be placed on the normalized resistance circles which all have one of their edges to the far right of the chart. The normalized reactance is to be placed on the reactance curves which all start from the far right of the chart. In this manner one can correctly place any impedance in the Smith chart, this is the starting point for any procedure to which you choose to use the Smith chart. To fully utilize the Smith chart it is important to talk about the admittance Smith chart, which can be thought of as the inverse of the impedance Smith chart. The admittance Smith chart uses conductance and susceptance as the real and imaginary parts of the admittance, respectively, where the admittance is the inverse of the impedance. For easier matching it is sometimes preferable to have the impedance and admittance Smith chart to overlap each other in one single Smith chart.

The ways one can match any impedance to any characteristic impedance is by using transmission lines, capacitors and inductors. Either way one chooses the end goal is all the same, to finally end up at the center of the Smith chart where the characteristic impedance is 1. Below will be given a brief guide in how matching is achieved using the earlier mentioned components.

If a transmission line is to be used the reflection coefficient for the line must be calculated, in most cases the reflection coefficient will be zero since the characteristic impedance of most transmission lines are designed to match the output of 50Ω. If the line is lossless the impedance in the Smith chart can be transformed by using a circle with origin at the center of the chart and radius $|\Gamma|$. Either by transforming to the right towards the generator or the left towards the load. The goal of using transmission lines is to end up on what is called the Smith chart help circles which are the circles where either the resistance is a constant of 1 in the impedance Smith chart or the constant conductance of 1 in the admittance chart. From there it is a matter of either using a capacitance or inductance for the final part of the matching. When using a capacitance the impedance transforms counter clockwise along a constant resistance circle in the impedance plane if added in series. If added in parallel it moves clockwise in the admittance plane. The case of adding an inductor is simply the opposite. How much an impedance transforms or moves along a certain circle is decided by the normalized impedance of the reactive component.

Chapter 3
Theory of AoA

3.1 Antenna Arrays

Antenna arrays can be used for various applications and measurements. They can both act as transmitters and as receivers depending on the application of use. Common in both situations is that the element spacing and phase between the elements plays a major part of the system. Element spacing introduces a time delay between the antenna elements which inherently turns into phase delay. This phase delay is used in both the transmitter and receiver applications.

3.1.1 Beamforming

As a transmitter an antenna array chooses the direction of the transmitted signal. This can be done through the combination of element spacing and phase delay of the antennas. Assume a Cartesian coordinate system of x, y, and z.. If two antenna elements are placed at $\pm\frac{d}{2}\hat{\boldsymbol{z}}$ and their respective radiation in the x-y plane they would constructively interfere with each other and the signal strength would increase. If a phase delay were to be introduced one could be able to change the constructive interference into destructive due to the fact that when antenna element one has a maximum antenna element two has could have minimum depending on position and through superposition the resulting signal would then be equal to zero. Figure 3.1 shows how the constructive interference maximum changes depending on a phase delay.

There are many possible ways to achieve maximas in certain directions. Some of the more popular methods are Schelkunoff's zero placement method, binomial method, Fourier series method, and Dolph-Chebyshev. Schelkunoff's zero placement method can be described with the formula

$$A(\theta) = \sum_{n=0}^{N} a_n z^n \tag{3.1}$$

where $z = e^{j\psi}$ and $\psi = kd\cos(\theta)$ and a_n is the weighting factor of the respective antenna element. The weighting factor determines the initial phase delay of the antenna elements. The result of this formula is the array factor which determines where the main lobes of the antenna array are located. Since it is possible to determine propagation direction through initial phase delay of the transmitting

antenna elements the opposite is also possible, that is, to determine the initial propagation direction through measured phase difference. If a certain initial phase delay of the transmitters results in a direction of θ then the same measured phase delay of the receiving antennas would tell us the direction from where the received was coming from.

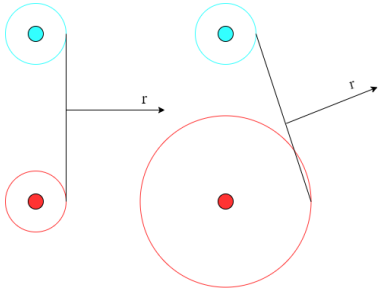

Figure 3.1: Direction of signal from a phase delayed antenna array.

3.1.2 Mutual Coupling

An effect of having antennas close to each other is mutual coupling. An antenna's radiation pattern and input impedance depends on the surface currents of the antenna element. By having two antenna elements close to each other rather than far away, they start to influence each other significantly which in turn causes the radiation pattern and the input impedance to change slightly. In the previous section beamforming was explained and how you can choose which direction the antenna array should transmit in. If the radiation pattern of the antennas change due to mutual coupling and this was not taken into consideration in the calculation the direction of the lobes might differ from the original value. Also if the input impedance changes the matching networks for which the antenna is connected to might not work as intended. Assume an antenna element with input impedance 50Ω were to be put into a module with 50Ω interface the reflection coefficient would be equal to zero. If however the input impedance would change due to mutual coupling the reflection coefficient would not be equal to zero which results in power and bandwidth losses which might be significant enough to render the system to not meet the required specifications.

Mutual coupling does not always have to be negative, since the effects of mutual coupling can be taken into consideration and the system can be tuned with mutual coupling in mind. Where the original antenna element would not meet the requirements but through mutual coupling it can behave according to the specifications. The effects of mutual coupling can be put into a mutual coupling matrix which can be used to tune the system with insufficient antenna elements to the desired effect.

3.1.3 Element isolation

In order to prevent mutual coupling from occurring there has to be isolation between the antenna elements [16]. The isolation can be done through many different methods. Two examples are putting isolating boundaries like walls between the elements, this approach enhance the performance of beam steering systems [17]. The other approach is slitting the ground plane in between the elements, this approach is applicable for non planar radiating systems as well as antenna arrays with a large number of arrays [18]. This stops the antenna elements to couple with each other hence not disturbing each other's surface currents.

3.2 Angle of Arrival

Angle of Arrival (AoA) is a measurement method for the direction of propagation of an incident wave onto an antenna array. AoA measurements can be done in two ways. Either through maximum signal power during antenna rotation or through phase difference between antenna elements. In this thesis the latter was used.

3.2.1 Phase difference

An incident wave is propagating towards an array of antennas of n elements with an angle θ this causes a phase shift of the received signal between antenna element 1 and antenna element n due to the extra propagating distance from the source to the respective antenna elements, as seen in Figure 3.2.

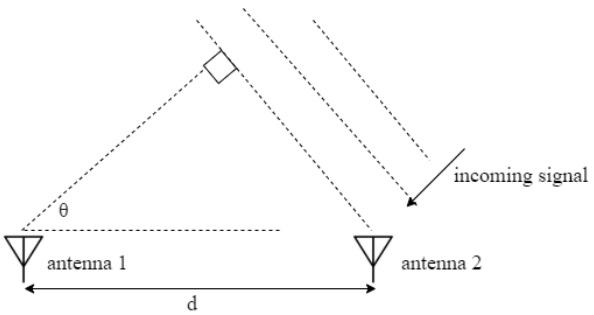

Figure 3.2: Theoretical setup of AoA measurement.

The magnitude of the phase shift depends on the spacing between the antenna elements and angle of incidence θ. The formula expressing the relation is

$$\theta = \arccos(\frac{\phi \cdot \lambda}{2\pi d}) \tag{3.2}$$

where ϕ is the measured phase difference, λ is the wavelength of the propagating wave, and d is the element spacing. Figure 3.3 is a plot for formula (3.2) it shows the relation between angle of incidence and measured phase difference between two different element spacings. The same measured phase difference would give us different angle of incidence for the two different element spacings. It is also worth

to notice that $\lambda/2$ provides a larger interval for the measured phase for the same amount of angle of incidence. This causes small errors for $\lambda/4$ to have a larger impact on the proposed incident angle than of the $\lambda/2$ system.

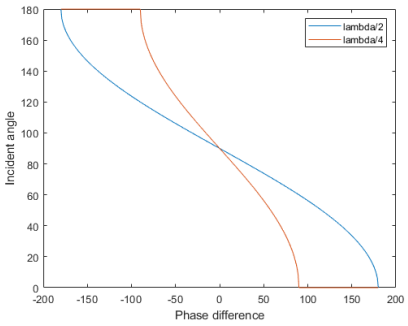

Figure 3.3: Difference between same measured phase difference between two different spacings.

Also if the spacing were to be larger than $\lambda/2$ aliasing would occur where the measured phase difference would correspond to two incident angles at the same time which causes the whole idea of AoA to falter as there is no way to distinguish which of the two hits is the correct one, this effect can be seen in Figure 3.4 where an incident angle of 30 degrees turns out to show two peaks, one at 30 degrees and one at -60 degrees. These peaks look identical and there is no way to tell which is the correct one. Since there is an upper bound of element spacing due to aliasing and a lower bound due to small errors resulting in false incident angles the optimal spacing for AoA becomes a trade off between how small one want the spacings to be and how sensitive the system should be.

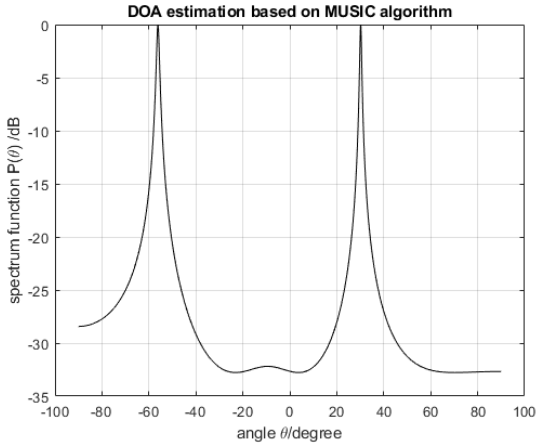

Figure 3.4: The effect of having spacing = 0.75λ. The real incident angle is 30 degrees but since the spacing is larger than 0.5λ aliasing occurs and there is no way to tell if the signal originates from +30 or -60 degrees.

3.2.2 IQ-Sampling

To give an overview of the concept of IQ-sampling we start of with the equation for a sine wave,

$$A\sin(2\pi f_c t + \phi), \tag{3.3}$$

where A is the amplitude of the signal, f_c is the frequency, and ϕ is the phase.

To encode information in the sine wave which is transmitted one is limited by changes in the above mentioned variables. The idea behind IQ-sampling is that the frequency and phase can be seen as the phase angle since the frequency represents the rate of change of the phase. With this information one can represent the instantaneous state of the sine wave with a vector in the complex plane represented by its amplitude and phase angle if plotted in a polar coordinate system as seen in 3.5.

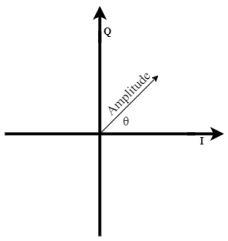

Figure 3.5: Polar representation of a sine wave.

The phase of the point in the plot changes according to the current state of the sine wave. To give an example if the frequency of the sine wave would be 1Hz the

dot would rotate around the origin (at constant radius if the signal has a constant amplitude) one revolution per second. This needs to be taken into account when sampling a signal of a certain frequency, in BLE 5.1 the frequency used is around 2.4 GHz as mentioned in section 2.1.1, the dot would then travel around the origin $2.4 \cdot 10^9$ times per second.

In practice IQ data is a translation of amplitude and phase data from polar coordinates to Cartesian coordinates using a simple trigonometric identity

$$A\cos(2\pi f_c t + \phi) = A\cos(2\pi f_c t)\cos(\beta) - \sin(2\pi f_c t)\sin(\beta) \tag{3.4}$$

from here set $I = A\cos(\phi)$ and $Q = A\sin(\phi)$ and we obtain

$$A\cos(2\pi f_c t + \phi) = I\cos(2\pi f_c t) - Q\sin(2\pi f_c t) \tag{3.5}$$

where I is the amplitude of the in-phase carrier and Q is the quadrature phase-carrier. When plotting the IQ-samples in a Cartesian coordinate system I is the real part and Q the complex.

3.2.3 Rayleigh Fading

Rayleigh fading is a phenomenon where the reflected waves give rise to an increase or decrease of amplitude on the measured signal compared to the expected amplitude through formulas such as Friis transmission formula as represented in Figure 3.6 where the black vector shows the measured signal while the first green arrow shows the actual sent signal and the other green arrows show how the reflections can effect the measured signal [19].

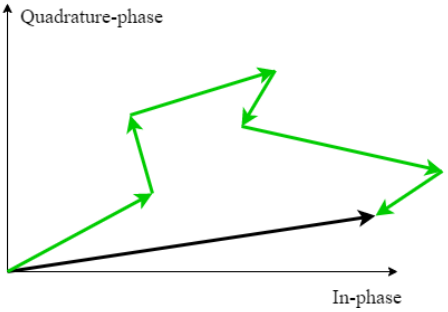

Figure 3.6: Representation of how reflected waves can effect measured signal.

The Rayleigh fading can be described as

$$R(t) = r \cdot cos(2\pi f_c \cdot t + \theta) \tag{3.6}$$

where r and θ can be described as random variables, their values vary with time as the waves reflect on the surroundings or with other changes as movement of receivers or transmitters [20]. Figure 3.7 shows how Rayleigh fading can impact

the received signal strength of a continuous wave transmitting on a receiver where they are both stationary.

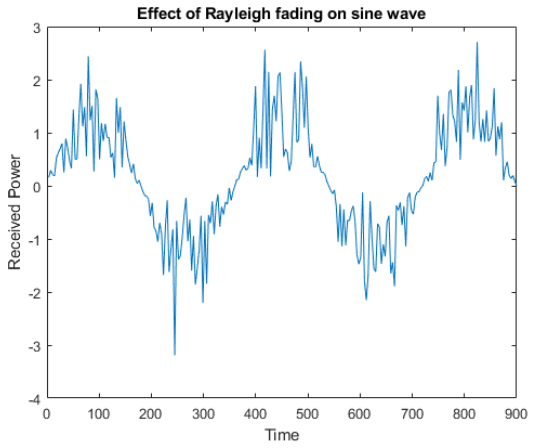

Figure 3.7: Representation of how reflected waves can effect measured signal.

The envelope of the received signal strength can be described statistically through the Rayleigh distribution whose probability density function is

$$p(r) = \frac{r}{\sigma^2} e^{\frac{-r^2}{2\sigma^2}} \tag{3.7}$$

where σ^2 = the average received power. If σ is normalized to $\sigma = 1$ the probability function can be seen in Figure 3.8.

Since this is a probability density function the area beneath the curve is equal to one. When integrating from $r = 0$ to $r = 1.253$ we get half the area, which means that there is a 50% chance that the received signal strength is below 1.253. The maximum of the curve is at the same value as σ. This function explains why Figure 3.7 had a lot of varying values around 0 dB (no change) but only a few big deviations as it is very uncommon for the received signal strength to become a lot higher (or smaller) than expected but it is very common for it to fluctuate around the expected value.

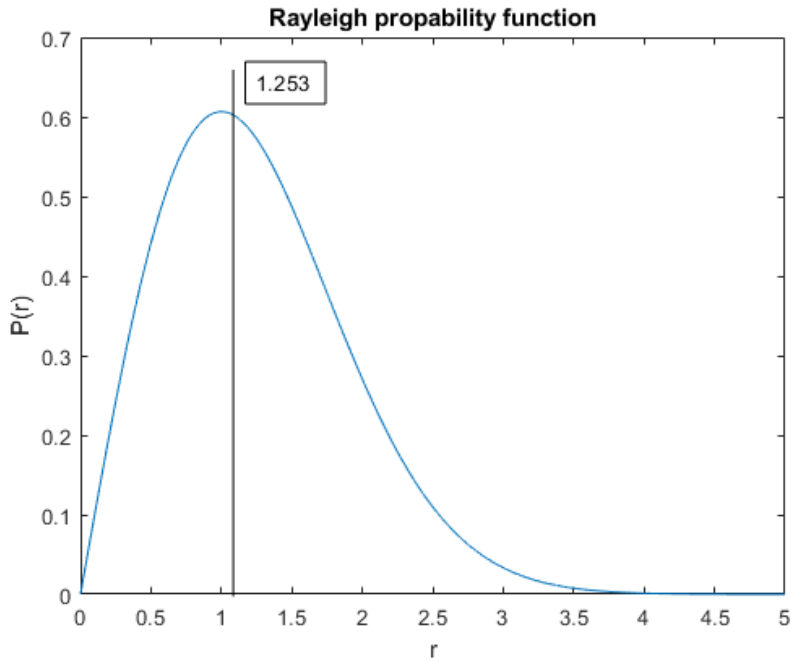

Figure 3.8: Probability density function.

3.2.4 MUSIC Algorithm

MUSIC (MUltiple SIgnal Classification) is an algorithm commonly used in AoA measurements as it works in uniform and non uniform linear arrays which means it is applicable in every linear antenna array. MUSIC depends on the covariance matrix between the different inputs in order to find which angle results in the highest covariance. It does this with the help of eigenvalue decomposition [21].

Assume an antenna array setup like Figure 3.9 where there are multiple incoming plane waves as well as an antenna array. D is the amount of incoming plane waves, M is the amount of receiving antenna elements and k is data sample and the spacing between the elements is d.

The direction of the incident signals is represented by the steering vector $a(\theta_i)$ where $a(\theta_1)$ would be the steering vector for signal 1. The steering vector $a(\theta_1)$ would in this case be

$$\begin{bmatrix} 1 \\ e^{j\beta dsin(\theta_1)} \\ e^{j2\beta dsin(\theta_1)} \\ .... \\ e^{j(M-1)\beta dsin(\theta_1)} \end{bmatrix}$$

where $\beta = \frac{2\pi}{\lambda}$ is the incident waves wave number and d = element spacing. This steering vector will become the first column in the upcoming A matrix, where

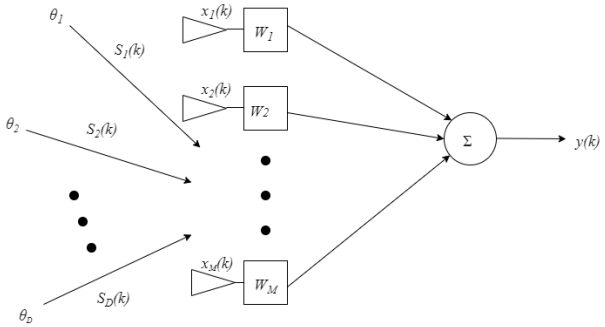

Figure 3.9: Antenna setup model for MUSIC.

the $a(\theta_2)$ would be the second column and so on until there are a total of D columns in the A matrix as follows.

$$\boldsymbol{x}(k) = \boldsymbol{A} \cdot \boldsymbol{S}(k) + \boldsymbol{n}(k) \tag{3.8}$$

$$\begin{bmatrix} \boldsymbol{x}_1(k) \\ \boldsymbol{x}_2(k) \\ . \\ . \\ \boldsymbol{x}_M(k) \end{bmatrix} = \begin{bmatrix} \boldsymbol{a}(\theta_1) & \boldsymbol{a}(\theta_2) & ... & \boldsymbol{a}(\theta_D) \end{bmatrix} \cdot \begin{bmatrix} S_1(k) \\ S_2(k) \\ . \\ . \\ S_D(k) \end{bmatrix} + \boldsymbol{n}_k$$

- $x_i(k)$ = amplitude of signal + noise in the ith element matrix size [M x K]
- $S_j(k)$ = vector of incident signal j at sample time k matrix size [D x K]
- $n_i(k)$ = noise vector at element i matrix size [M x K]
- $a(\theta_i)$ = array steering vector [M x 1]
- A = matrix of steering vectors, [M x D]

The correlation matrix is given by

$$\begin{aligned} R_{xx} = E[x \cdot x^H] &= E[(AS + n)(S^H A^H + n^H)] \\ &= AE[S \cdot S^H]A^H + E[n \cdot n^H] = AR_{SS}A^H + R_{nn} \end{aligned} \tag{3.9}$$

The correlation matrix has M eigenvalues along with M associated eigenvectors $E = (e_1 e_2 .... e_M)$. If the eigenvalues were to be sorted from largest to smallest one could divide the matrix E into two subspaces $[E_N E_S]$ The first subspace E_N is called the noise subspace and is composed of $M - D$ eigenvectors associated with noise and the second subspace E_S is called the signal subspace where the eigenvectors are associated with the signals. Lastly the noise subspace eigenvectors are orthogonal to the array steering vectors at the angle of incidence of the signals 1-D because of this condition it is possible to show that the Euclidian distance

$d^2 = a(\theta)^H E_N E_N^h a(\theta) = 0$ for each and every incident angle. Putting this product in the denominator creating the expression

$$P_{\mathrm{MU}}(\theta) = \frac{\boldsymbol{a}(\theta)^H \cdot \boldsymbol{a}(\theta)}{\boldsymbol{a}(\theta)^H \boldsymbol{E}_N \boldsymbol{E}_N^H \boldsymbol{a}(\theta)} \tag{3.10}$$

would create large peaks at the incident angles [22].

Chapter 4
Software and Hardware Tools

4.1 Hardware tools

The main use of the hardware tools in this thesis has been to transmit data to antennas under use to later be examined using software tools.

4.1.1 Transmitter and receiver

The Nordic semiconductor chips shown in Figure 4.1 are used as both receivers and transmitters for all AoA measurements. The exact chip used is the nRF52 DK Nordic semiconductor ship [23]. These chips are programmable and are built upon circuit boards with antenna compatibility. The chips have the option to gather and send data crucial for AoA measurements with good precision and bitrate for the systems at use.

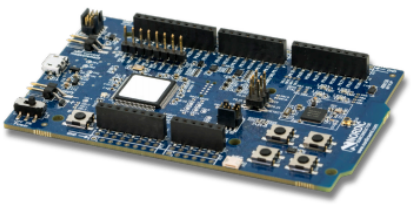

Figure 4.1: Picture of the Nordic transceiver.

4.2 Software tools

Many different software tools have been used during the work ranging from calculation tools to software for programming the transmitters and the receiver circuits. IQ-data has been sent, sampled and used to calculate the angle of arrival. The programs used to achieve all of this are listed below.

4.2.1 SEGGER

SEGGER is a software tool for programming the Nordic semiconductor chips [24]. SEGGER tells the transmitter and receiver how to behave and what to send. The transmitter settings were not changed during the work and all the changes were on the receiver circuit. The settings mainly changed on the receiver were switching pattern and number of samples per signal period. Changing the switching pattern of the antenna array is crucial to determining AoA in BLE 5.1 as having the three antenna elements simultaneously listening consumes more power than only having one listening at a time. The IQ-data from SEGGER is a long array of values where the first value is an I value and the second is a Q value alternating until the transmission is over. After 32 IQ pairs the element switching occurs which means that the first 64 values are the IQ-data from antenna element 1 while the next set of 64 values are the IQ-data from antenna element 2. The total amount of IQ pairs in a transmission are 1120 which are split up into 35 antenna samples as $\frac{1120\,\text{IQ pairs}}{35\,\text{samples}} = 32\,\text{IQ pairs/sample}$. How these 35 are divided on the antenna elements depends on the switching pattern of the SEGGER code. Due to error prevention schemes used in the code the final samples obtained are 33 antenna samples with 16 IQ pairs each.

4.2.2 PuTTY

PuTTY is a software that supports several network protocols [25]. We used it to transfer the received IQ-data from an antenna element. In this case the data shown in PuTTY are the IQ samples sent from the transmitter to the receiver. PuTTY displays the array of values sent from the SEGGER code in a terminal window where it is easy to extract the data into a calculation tool.

4.2.3 Matlab

Matlab is a program used for mathematical and technical calculations. It is based on arrays and matrices which makes it a perfect fit for our work [26].

4.2.3.1 Matlab Measurements

The sampled IQ-data from SEGGER and PuTTY were imported into Matlab where the long array of 2240 values (1120 pairs) were reshaped and reordered into a matrix where each column represent an antenna sample see Appendix A where antenna sample 3 is reformed from array to matrix. After all the error prevention IQ pairs have been removed from the input data, the data is put into the MUSIC algorithm which compares each antenna element with each other and figures out the phase difference between them. This phase difference is then used to calculate the angle of incidence according to section (3.2.1). A plot of the results of a measurement is shown in Figure 4.2. The plot shows that the angle of incidence of the signal is -27.1 degrees which means that the phase difference in Equation (3.2) was $\approx +100$ degrees.

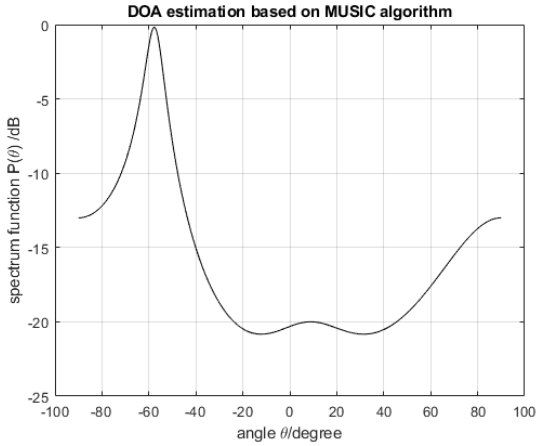

Figure 4.2: Results of 30 degree incident angle measurement.

4.2.3.2 Matlab Simulations

Matlab was also used to simulate how well the MUSIC algorithm performs with a synthetic signal rather than a measured one in order to study how noise and other impairing effects such as Rayleigh fading affect the AoA performance of the system compared to the synthesised one. Basically the difference between the measured values and the synthetically generated values can be achieved and then check what kind of impairing effects give rise to such deductions in order to find which impairing effect is the most present one.

4.2.4 HFSS

HFSS is a software tool used for antenna design and RF circuitry [27]. It allows the user to create any design and simulate its performance, it could be single antenna elements or entire arrays. HFSS was mainly used to check the performance of various antenna array setups, for example how the mutual couplings between the antenna elements depend on the spacing between them. Being able to get the radiation patterns of antenna elements were also of great use as the AoA measurements is greatly dependent on the radiation pattern. A lot of time was spent in HFSS designing an antenna array, where dimension, layering, antenna placement, feed positions and transmission lines were built in order to achieve the specifications. In HFSS it is possible to get voltages, currents, power, impedance values, S-parameters, their respective phases, radiation patterns as well as being able to visiualize E-fields and radiation patterns in 3D, all of these possible results makes it a very powerful tool in order to tune and analyze antenna performance.

Chapter 5
Method

The method used to achieve a size reduced shield for AoA measurements can be broken down into three major steps: measurements of AoA on a basic prototype, compare those results with theoretical result, and designing new and improved prototype in simulation software. First the physical measurements were done to measure how well we are able to measure AoA. Then some sort of theoretical values are needed to make it possible for us to compare our measured values with the theoretical ones in order to find out how much the impairing effects actually decrease performance. The theoretical values were generated through synthetical signals in matlab. Typically outer angles and tighter spacing increases the measurement error. With these two sets of result and an accepted margin of error a decision can be made where a spacing has lower errors than the accepted error of 5 degrees for a certain field of view. For example 0.25λ has lower than the accepted error for angles 60-120 degrees, whereas 0.5λ has lower than the accepted error for angles 40-140 degrees, a wider field of view. In order to be able to pick a spacing a field of view and error requirement has to be set and with these requirements the smallest spacing that fulfills these requirements is the chosen spacing used further down the design.

The next step is to build the shield in a simulation software in order to test out the antennas individual performance and tune the antenna element so that they perform the intended way with the impairing effects the simulation software introduces. Here it is important to include as many things as possible to tune the antennas with as many impairing effect as possible, i.e., adding transmission lines, switches and having a finite ground plane. When the antenna elements are matched and have good radiation patterns on each of the possible excitations, production can begin and a prototype can be manufactured.

5.1 IQ-samples

In order to be able to read IQ samples two different softwares were used, SEGGER and PuTTY. SEGGER allowed us to control the switching of the receiving antenna array, packaging format, amount of samples and switching time. This allowed us to be able to sample the 250kHz wave that is created by the IQ pairs and obtain 16 IQ pairs on half a wavelength of the 250kHz wave before the switch-

ing occurred and the next antenna could take 16 new pairs. A fast switching time is crucial for AoA measurements that depend on switching if it is very slow the switching time may overlap with the upcoming sampling. When everything is setup the transceiver sends the CTE-tone towards the receiving antenna array and PuTTY reads the IQ-samples gathered and puts them in a terminal window on the computer. These values were then put into Matlab and reshaped so that they fit our algorithm. Matlab would then run the MUSIC algorithm to show a spectrum from -90 to 90 degrees with peaks at incident angles found from the IQ-samples. The position of the peak (not the amplitude) was then taken as the measured angle.

The Matlab code used for AoA estimation that took our IQ samples as input and ran them through our MUSIC algorithm was written from scratch. Firstly we had to know which values from PuTTY were I respectively Q values, this was explained in section 4.2.1, every other value is an I respectively Q value and a set of 32 IQ values was from antenna one and the next set of 32 was from antenna two. An IQ sample would end up on the form

$$[I_{1,1}Q_{1,1}I_{1,2}Q_{1,2}...I_{1,j}Q_{1,j}I_{2,1}Q_{2,1}...I_{1+(i-1)\mathrm{mod}(e),j}Q_{1+(i-1)\mathrm{mod}(e),j}] \tag{5.1}$$

where i is the IQ set number, j is the sample number and e is the number of antenna elements used in this specific switching pattern. We know that each set is per antenna switching which means that the switching pattern used impact which set belongs to which antenna. In our physical measurements the first set is from antenna one, the second set from antenna two, the third set from antenna three and this repeating for the remaining 30 sets.

Editor - Music.m

Input A

32x33 complex double

	1	2	3	4
1	-9.5000e+01 - 1.5200e+02i	-1.6400e+02 - 3.0700e+02i	-6.6300e+02 + 2.2000e+01i	-5.0400e+02 - 1.7500e+02i
2	-6.2000e+01 - 1.6500e+02i	-2.2000e+02 - 3.9400e+02i	-5.6700e+02 - 1.2400e+02i	-3.7000e+02 - 1.5900e+02i
3	-2.6000e+01 - 1.7100e+02i	-2.8700e+02 - 4.8600e+02i	-4.5000e+02 - 2.7100e+02i	-2.2700e+02 - 1.2500e+02i
4	1.1000e+01 - 1.7000e+02i	-3.4600e+02 - 5.7600e+02i	-3.2500e+02 - 4.0800e+02i	-90.0000 - 81.0000i
5	4.7000e+01 - 1.6300e+02i	-3.7800e+02 - 6.6000e+02i	-1.9700e+02 - 5.2700e+02i	27.0000 - 37.0000i
6	8.2000e+01 - 1.4900e+02i	-3.6800e+02 - 7.3300e+02i	-7.2000e+01 - 6.1500e+02i	1.1400e+02 + 2.0000e+00i
7	1.1400e+02 - 1.3000e+02i	-3.0900e+02 - 7.8500e+02i	4.6000e+01 - 6.6700e+02i	1.6600e+02 + 2.9000e+01i
8	1.3900e+02 - 1.0500e+02i	-2.0100e+02 - 8.1300e+02i	1.5700e+02 - 6.7600e+02i	1.8300e+02 + 4.6000e+01i
9	1.5900e+02 - 7.4000e+01i	-4.8000e+01 - 8.1200e+02i	2.6400e+02 - 6.3900e+02i	1.7000e+02 + 5.6000e+01i
10	1.7000e+02 - 4.1000e+01i	1.3200e+02 - 7.8300e+02i	3.6700e+02 - 5.6100e+02i	1.3900e+02 + 6.7000e+01i
11	1.7500e+02 - 6.0000e+00i	3.1900e+02 - 7.2500e+02i	4.6500e+02 - 4.5000e+02i	1.0000e+02 + 8.2000e+01i
12	1.7100e+02 + 2.9000e+01i	4.9300e+02 - 6.4400e+02i	5.5500e+02 - 3.1600e+02i	6.2000e+01 + 1.0400e+02i
13	1.5900e+02 + 6.4000e+01i	6.3500e+02 - 5.3800e+02i	6.2800e+02 - 1.7100e+02i	3.0000e+01 + 1.2800e+02i
14	1.4200e+02 + 9.6000e+01i	7.3500e+02 - 4.1300e+02i	6.7500e+02 - 2.5000e+01i	8.0000e+00 + 1.5200e+02i
15	1.1900e+02 + 1.2500e+02i	7.9000e+02 - 2.6800e+02i	6.8800e+02 + 1.1600e+02i	-9.0000e+00 + 1.7000e+02i
16	9.1000e+01 + 1.4900e+02i	8.0600e+02 - 1.1000e+02i	6.6600e+02 + 2.4900e+02i	-2.7000e+01 + 1.7700e+02i
17	6.0000e+01 + 1.6500e+02i	7.8900e+02 + 5.5000e+01i	6.0700e+02 + 3.7000e+02i	-4.8000e+01 + 1.7200e+02i
18	2.7000e+01 + 1.7500e+02i	7.4400e+02 + 2.1900e+02i	5.1900e+02 + 4.7800e+02i	-7.4000e+01 + 1.5800e+02i
19	-7.0000e+00 + 1.7700e+02i	6.7800e+02 + 3.7300e+02i	4.0600e+02 + 5.6800e+02i	-1.0100e+02 + 1.3500e+02i
20	-4.3000e+01 + 1.7100e+02i	5.9100e+02 + 5.1000e+02i	2.7900e+02 + 6.3700e+02i	-1.2800e+02 + 1.0700e+02i
21	-7.5000e+01 + 1.5800e+02i	4.8100e+02 + 6.2300e+02i	1.4300e+02 + 6.7900e+02i	-1.5100e+02 + 7.7000e+01i
22	-1.0700e+02 + 1.3900e+02i	3.5000e+02 + 7.0900e+02i	1.0000e+00 + 6.9300e+02i	-1.6700e+02 + 4.5000e+01i
23	-1.3200e+02 + 1.1500e+02i	2.0200e+02 + 7.6600e+02i	-1.4100e+02 + 6.7500e+02i	-1.7400e+02 + 1.1000e+01i
24	-1.5400e+02 + 8.5000e+01i	4.3000e+01 + 7.9300e+02i	-2.7700e+02 + 6.2800e+02i	-1.7300e+02 - 2.3000e+01i
25	-1.6700e+02 + 5.3000e+01i	-1.1800e+02 + 7.9000e+02i	-4.0500e+02 + 5.5300e+02i	-1.6600e+02 - 5.7000e+01i
26	-1.7400e+02 + 1.9000e+01i	-2.7500e+02 + 7.5700e+02i	-5.1700e+02 + 4.5500e+02i	-1.5200e+02 - 9.0000e+01i
27	-1.7300e+02 - 1.8000e+01i	-4.2000e+02 + 6.9800e+02i	-6.0700e+02 + 3.4000e+02i	-1.3300e+02 - 1.1900e+02i
28	-1.6600e+02 - 5.3000e+01i	-5.4800e+02 + 6.1300e+02i	-6.7200e+02 + 2.1300e+02i	-1.0800e+02 - 1.4100e+02i
29	-1.5200e+02 - 8.7000e+01i	-6.5300e+02 + 5.1200e+02i	-7.0800e+02 + 8.4000e+01i	-7.7000e+01 - 1.5800e+02i
30	-1.3500e+02 - 1.2400e+02i	-7.2400e+02 + 4.0000e+02i	-7.1300e+02 - 3.1000e+01i	-4.1000e+01 - 1.7500e+02i
31	-1.2400e+02 - 1.7000e+02i	-7.5100e+02 + 2.8300e+02i	-6.8300e+02 - 1.1600e+02i	0.0000e+00 - 2.0100e+02i
32	-1.3100e+02 - 2.3000e+02i	-7.2900e+02 + 1.5900e+02i	-6.1200e+02 - 1.6400e+02i	3.9000e+01 - 2.5500e+02i

Figure 5.1: IQ sets.

Figure 5.1 shows the formatting while the IQ samples have been imported and reshaped into Matlab. Here each row is an IQ sample with I being the real part and Q being the imaginary part. The first 16 IQ pairs per antenna are also not used as the first pairs of this group of 16 might be affected by the antenna switching which will compromise accurate AoA measurements. All in all the total removal of IQ pairs results in the 32×35 matrix to be reduced to 16×33 matrix where the 16 rows are rows (17→32) in the original matrix and the 33 columns are columns (3→35) in the original matrix.

The next step is to put all of these IQ samples into the MUSIC algorithm. Note that the implemented algorithm only takes 1 out of the 11 total laps per time it is used, which means that it uses columns (1,2,3) then (4,5,6) and so on until (31,32,33). This means that we have to create some sort of average as the transmission might be different between these 11 different laps of sampling. This was done through finding the degree spectrum for columns (1,2,3), (4,5,6) until all columns had gone through the algorithm and adding all of these spectrum's together and taking an average. The reason why we did not take an average of the IQ data before the algorithm was due to the fact that the IQ data tended to start at different angles for every lap which is not a concern when taking the average of the results of each lap but does become a problem if we were to take an average on the IQ data itself. This should result in peaks that appeared on different incident angles due to bad transmissions getting averaged out and the true incident angle making it through the averaging (note that in this specific step the spectrum is logarithmic and adding in logarithmic scale is the same as multiplying in linear which should remove the bad peaks very quickly). Figure 5.2 shows how the averaged spectrum looks like while Figure 5.3 shows the spectrum of lap number four, it is noticeable that the averaged spectrum is closer to the middle than lap number 4 which means that the averaged one had more contributions closer to zero or more to the left of the middle than right. Therefore we can conclude that it is important to have an average per transmission rather than to only take one value out of the transmission. It is also worth mentioning that the measured angle is the top of the peak and there was no consideration of how wide the peak was when extracting the angle of incidence from the measured data.

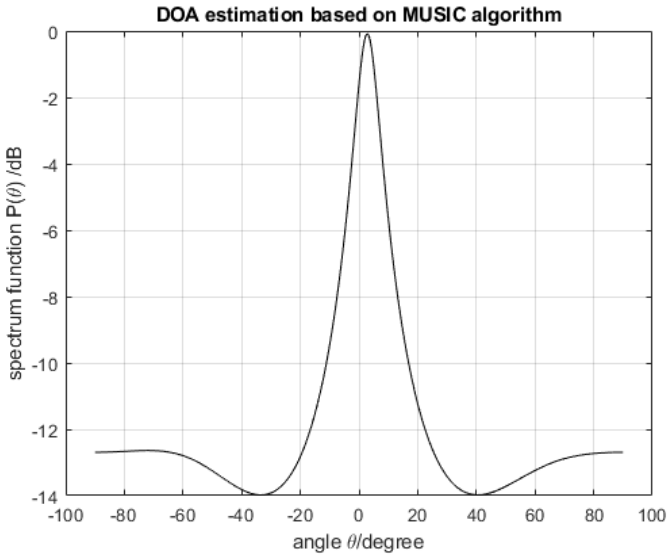

Figure 5.2: Averaged degree spectrum of all 11 rounds. Taken from the physical measurements with element spacing 0.5λ.

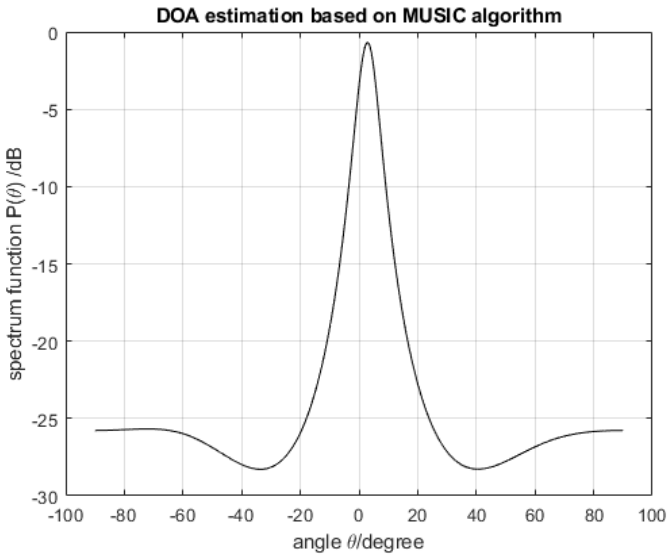

Figure 5.3: Degree spectrum of round number 4 out of the total 11. Taken from the physical measurements with element spacing 0.5λ.

5.2 Physical measurements

The measurements setup used for the physical measurements were having the antenna elements connected to the Nordic receiver circuit and applying the switching pattern. They were put at different spacing's ranging from $0.25\lambda(3.07\,\text{cm})$ to $0.5\lambda(6.14\,\text{cm})$ in steps of $0.025\lambda(3\,\text{mm})$ giving a total of 11 different spacing tested. The transmitter was a horizontally polarized antenna element and the receiving antennas were oriented horizontally for maximum received power. The transmitter was moved along a half circle over the receiving antenna array as seen in Figure 5.4. The transmitting antenna was placed at the desired angle and the three receiving antennas were placed at the bottom of the half circle and straight under the 90 degree marker.

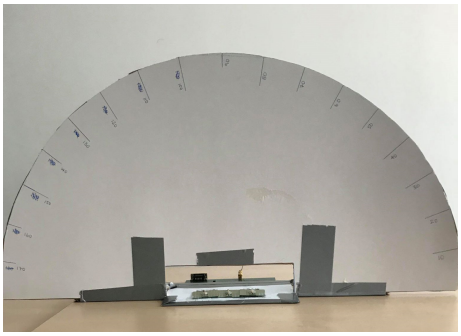

Figure 5.4: Physical setup for AoA measurements with Nordic receiver and transmitter.

The measurements were taken across the entire half circle in 10 degree steps starting at 10 degrees, ending at 170 degrees. This in total gives 17 transceiver placements. Every angle had 10 sets of IQ samples in order to make sure that an average could be taken. All in all $17 \cdot 11 \cdot 10 = 1870$ sets of IQ samples were taken and put into the MUSIC algorithm. The results from the IQ samples were compared with synthetic signals put into the same MUSIC algorithm to try to find some correlations and similar behavior. When all 1870 sets of IQ samples had been gathered each and every set of IQ samples went through the Matlab code described in Section 5.1.1. All of the peak positions in the spectrum were stored away in excel files and gathered to later be analyzed in order for us to find which spacing performed the best. Note that all the 1870 IQ sets were gathered before they were imported into the Matlab code. If in the final excel spreadsheet we would find a deviation far greater than what would be expected, say that 8 out of 10 measurements were good while 2 deviated so much that the average error would exceed 15 degrees from the previous angle the measurement for that specific angle would be retaken. Except for the outer angle cases as these will usually have very large errors. If it then performed better, that result would be used instead of the previous one. It is worth mentioning that only one additional measurement was done for the angles that had angle deviations that impacted the average in a too negative way. This was done in order to have as fair measurements

as possible for all angles, and not simply have measurements taken until a desired result was achieved. An example is given in Figure 5.5 where one of the angles for the incident angle of 60 degrees gives the error of 90 degrees whereas the rest of the measurements generated an error of around 20 degrees. Here ten new measurements were taken and one of the measurements were used randomly to correct the faulty measurement, giving a more just average.

50		60	
angle	error	angle	error
-43.7	-3.7	63.3	93.3
-42.9	-2.9	-50.2	20.2
-42.2	-2.2	-50.9	20.9
-43.9	-3.9	-52.9	22.9
-43.6	-3.6	-48.4	18.4
-43.6	-3.6	-48.4	18.4
-43.7	-3.7	-48.2	18.2
-42.9	-2.9	-48.9	18.9
-42.2	-2.2	-49.1	19.1
-43.9	-3.9	-49.4	19.4
-43.26	-3.26	-44.64	29.9666

Figure 5.5: Example of excel file consisting of measured angles of different incoming angles at a spacing of 0.35λ between antenna elements.

5.3 Synthetically generated data

To gain a better understanding in what performance could be expected from the antenna array it was necessary to perform a synthetic or ideal test of the setup. The reasoning for this is to find the best elements spacing under ideal conditions to compare with the physical measurements to gain understanding of what angle estimation errors could be expected. If for example the simulated measurements gave a certain angle estimation error the physical measurement should not be able to estimate the incident angle with a smaller error. This was done using matlab where a generated signal was created in every antenna element to represent ideal conditions. In order to recreate the physical measurements as well as possible some scalable parameters were necessary. These were parameters in Friis transmission formula such as gain, distance and transmitted/received power, as well as antenna element spacing and angle of incidence. The latter two were made into vectors containing all element spacings used in the physical measurements as well as angles of incidence ranging from 0 to 180 degrees with 5 degree steps.

Each element in the array had a specific signal created for it, this was to resemble the actual received signal the elements received in the physical measurements. To mimic the physical test the generated signals given to the elements could not be continuous since the physical measurements samples signals and obtains 16 samples per measurement per element. The generated signal was also made to only consist of 16 samples of an ideal continuous wave to mimic the physical measurement setup. In Figure 5.7 and 5.6 the signals for both the synthetically generated data and the experimentally measured data are shown. Note that the generated one resembles a half circle more than the physical one. This is due to that the generated signal is under ideal conditions. To better represent reality some more parameters are needed, these are polarization mismatch loss, Rayleigh fading and noise. The polarization mismatch loss is needed since as the transmitter approaches the outer angles the polarization mismatch increases, due to the transmitter and receiver being matched at 90 degrees (the transmitter is straight above the receiver) and when the transmitter is moved along the half circle the orientation follows the circumference of the half circle and the total received power decreases resulting in inconsistent measurements, as mentioned this is dependent on angle and acts as a scalar for the received power. The parameter was added to each antenna element separately. Once these operations were performed an input vector was created consisting of the three antenna elements signals.

The other two scalable impairing effects, Rayleigh fading and noise, were added to the whole input vector. These two effects had a large impact on the measured signal and can be seen in 5.8. As seen the two effects impacts amplitude and in turn distorts the signal to quite an extent and this in turn effects the results in a great way. Having the Rayleigh fading too large would corrupt the input as well as having to great of a noise floor would have the algorithm not distinguish signal from noise. To have as fair as possible synthetically generated data these effects were scaled to resemble reality and since neither the impact of Rayleigh fading in the physical measurements could be measured or the SNR in the physical mea-

surements was known the parameters were tuned to resemble reality. The constant parameters used that do not change throughout the measurements are shown in Table 7.1. The noise was the easiest one to adjust since it was all dependent on the signal power, therefore typical antenna values for gain and transmitting/receiving power were added to the signals.

Once all of the above was performed, an input vector was the result which was run through the MUSIC algorithm which exported the results in form of angle estimation error in a matrix. The algorithm was performed for each incoming angle at each different spacing 100 times using a loop function until ultimately an average was taken and exported into an excel matrix. The matrix was then examined in the same fashion as the physical measurement result matrix to find the field of view for each antenna element spacing.

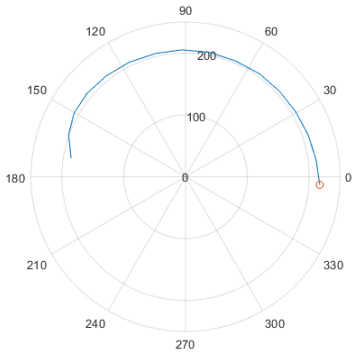

Figure 5.6: Physical measured IQ data for one IQ set.

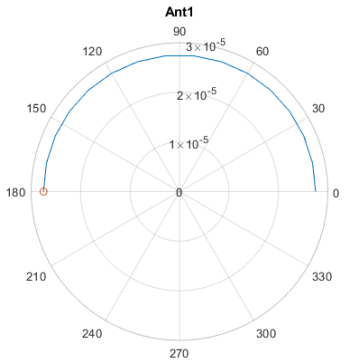

Figure 5.7: Synthetically generated IQ data for one IQ set.

The theoretical noise floor was designed to alter the IQ samples with both a real and imaginary part. The value of the alteration's is the noise floor level. This

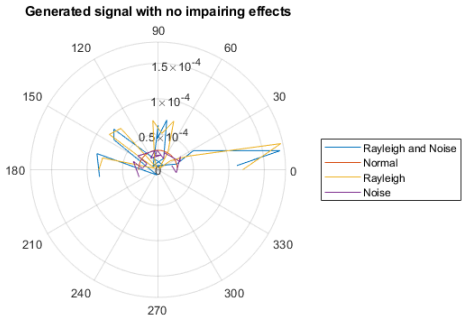

Figure 5.8: Comparison of synthetically generated IQ data with added noise, Rayleigh fading and both noise and Rayleigh fading active.

was done through adding on the white noise's real and imaginary part on top of the signals real and imaginary part which then randomly changed the IQ values of the signal as seen in Equation 5.2.

$$\begin{aligned} IQ_{\text{noise+signal}} &= IQ_{\text{noise}} + IQ_{\text{signal}} \\ r_{\text{signal+noise}} e^{j(\theta_{\text{signal+noise}})} &= r_{\text{signal}} e^{j(\theta_{\text{signal}})} + r_{\text{noise}} e^{j(\theta_{\text{noise}})} \end{aligned} \tag{5.2}$$

5.4 HFSS

Once a result had been achieved from both the simulated and actual AoA measurements the design of the shield could begin. The first step is to choose an antenna, our chosen antenna was a quadratic patch antenna with a starting geometry of $29\,\text{cm} \times 29\,\text{cm}$ and thickness of $34\,\mu\text{m}$. This was tuned later on in the process but was considered a good starting point for the shield design. It was decided that the shield should be able to gather AoA measurements in two dimensions, elevation and azimuthal, this requires at least two differently oriented linear arrays present in the design. An L shape was chosen as this uses the same antenna element twice which is optimal when trying to save space aswell as containing two linear arrays. Figure 5.9 shows a picture of the design in HFSS. A T shape could also be used as this has many of the same properties as the L shape but did not leave as much free space left on the shield for other necessities as switches and equidistant transmission lines and therefore was not chosen. Note that the pairs (5,6) and (9,10) are not symmetrical to the others in their respective row but the rows in themselves are symmetrical. This might have to be compensated for in the software that will use this shield but this will not be further discussed in this thesis.

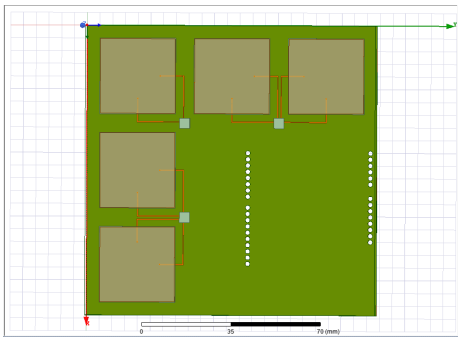

Figure 5.9: L shape design of shield in HFSS.

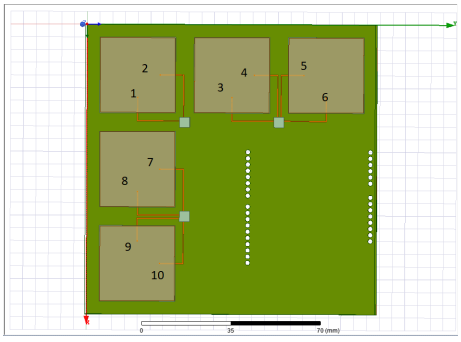

Figure 5.10: L shape design of shield in HFSS, numbered.

Figure 5.10 shows all the possible ways of switching and exciting the antennas. Each antenna element is cross polarized which makes the shield able to check both linear arrays in two polarizations for the best possible reception. Assume the shield to be placed along a wall then the horizontally oriented linear array would be able to measure the azimuthal angle through feeds 1,3 and 6 and the vertically oriented array will then measure the elevation angle through feeds 1,8 and 9. If the reception ends up being too bad for an accurate measurement a polarization switch could be of use in order to increase the reception strength and once again have accurate AoA measurements which would change the feeds used to 2,4 and 5 for the horizontal array and 2,7 and 10 for the vertical array. All of these switches will be handled by another software program and will not be implemented in HFSS.

With antennas chosen and all possible feed points figured out the next step is to build the shield and on top of that add the antennas in their desired positions. There are a total of five layers used in the shield design. Layer 1 is a 46 μm thick layer of FR4, layer 2 is a 34 μm thick layer of copper, layer 3 is a 1854 μm thick layer of FR4, layer 4 is another layer of FR4 which is 1600 μm thick and lastly layer 5 which is the patch antenna at 34 μm copper. Figure 5.11 shows the profile shield, note that these thicknesses were taken from an older project provided by u-blox.

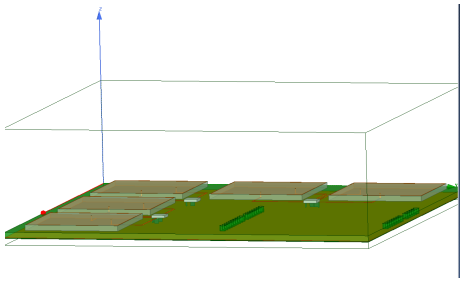

Figure 5.11: Profile of the shield design.

From this point all that is left is the tuning of the antenna elements to make sure each antenna element as well as their respective feeds all work at the bluetooth frequency, has a sufficient bandwidth and that the radiation pattern is as close to an omnidirectional radiation pattern as possible. The parameters tuned in order to achieve this was the width and length of the antenna elements, the feed positions, edge spacing (how far from the edge of the ground plane each antenna is positioned). The reason why the previously working antenna element now has to be tuned is due to the impairing effect of the shield's design, now many antennas are close together and sharing a non finite ground plane which will alter their performance and this has to be taken into account or the antennas will not perform as intended.

In order to test which setup of the previously mentioned parameters performs the best was done through simulating a single feed point for example feed number 7 and running the simulation over and over again through many permutations of the parameters. Up until the S11 parameter reached the point of meeting the

requirements set as well as the radiation pattern being omnidirectional. This was done through the Analyze all feature in HFSS and setting up results for S11, Impedance and Radiation pattern. Figures 5.12, 5.13, and 5.14 show how these results were presented in HFSS. For the S11 graph markers were put at 2.4GHz (bottom of spectrum), 2.44GHz(middle of spectrum) and 2.48GHz(top of spectrum) and if all markers met the requirements which is S11 being below -10dB for the entire spectrum for a specific setup of parameters they would be considered viable choices for the shields design. If the impedance is relatively close to achieve a real part of 50 Ohms and 0 reactance and met the S11 requirements then it was time to check if the radiation pattern looked sufficient. The method to checking if the radiation pattern was sufficient was to simply have HFSS plot it in a 3D polar plot and manually check if there were any specific angles that did not have enough gain set by the requirements which in this case was to have a field of view of 100 degrees, this could also be done by plotting the radiation pattern in a 2D plot and scanning through all the azimuthal angles and setting up markers where the radiation pattern is at its lowest gain and check if any of these are below the requirements.

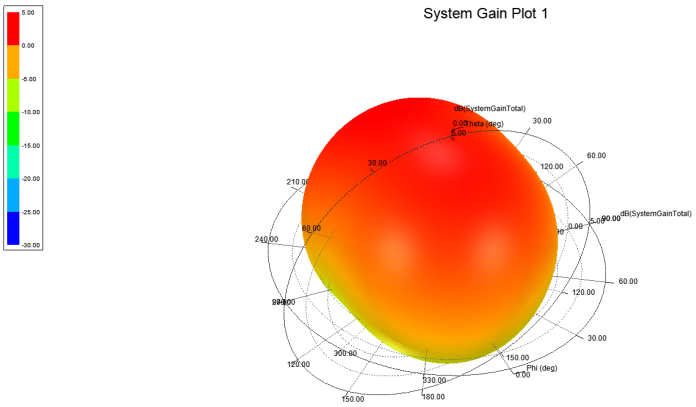

Figure 5.12: Example radiation pattern.

When all the requirements were met on a single excitation all the other nine excitations were then tested with the same parameters and if all of the excitations met the requirements then that specific setup of parameters was chosen for the shield's design. All in all, first one excitation was tested and when that one met the requirements all others were tested and if all met the requirements then those parameters will be used. Note that all the 5 antennas are the same size and the two antenna arrays are symmetrical as symmetry and consistency is important for AoA measurements which is why it was so important to test all of the excitation's rather than just one even though it could be seen as trivial if one works all should work due to the symmetry.

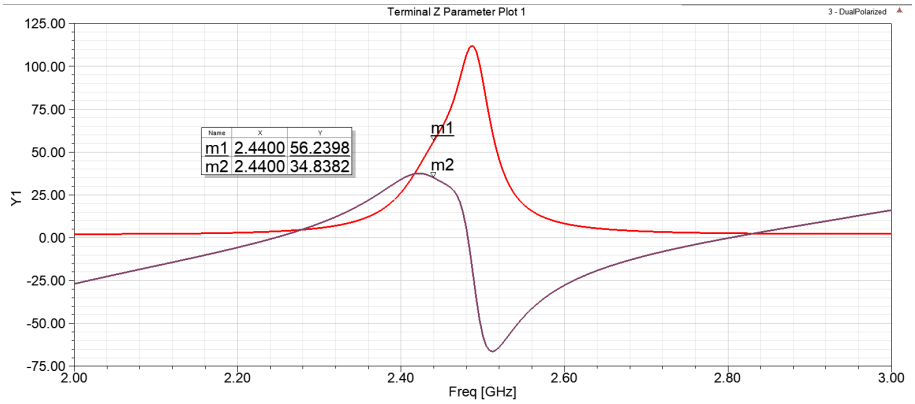

Figure 5.13: Example impedance results. Red line is the real part and purple is the imaginary part.

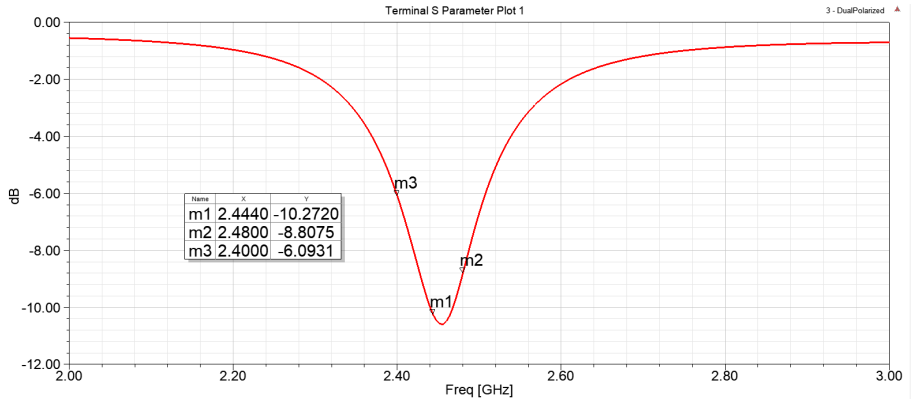

Figure 5.14: Example S11 results.

When tuning the antennas to meet the requirements feed position would be the first parameter to tune since this parameter does not change the overall size of the shield, if edge spacing or antenna size change the total length and width of the shield changes with the formula

$$\text{Total length} = 2 \cdot \text{edge spacing} + \text{antenna length} + (\text{elements} - 1) \cdot \text{spacing}$$

and the same formula applies for total width as the shield is meant to be quadratic. Therefore antenna dimensions and edge spacing would only be altered when the requirements could not be met through only altering the feed position. In that case antenna dimensions would be next in line to be altered as it would turn out that small changes to the antenna dimensions impacted the results more than the same size of altering with edge spacing.

5.4.1 Altered Layering

The parameters found in HFSS were used by our company supervisor to build the shield in Allegro, however due to manufacturing the layering had to be altered and thus altering the tuning of the parameters. This made it so that we could no longer compare the simulated results with the measured results for the shield and thus a second round of simulations were done in order to be able to compare the two. Figure 5.15 shows the new set of layers used in the shield. Note that the only thing that has changed are the layers (Z-direction) and all the parameters used for the tuning (XY-direction) are the same as in the previous section. All the copper layers used in the layering are $35\mu m$ whilst the substrates total height are $1470\mu m$ thick thus making the total height of the shield $3080\mu m$.

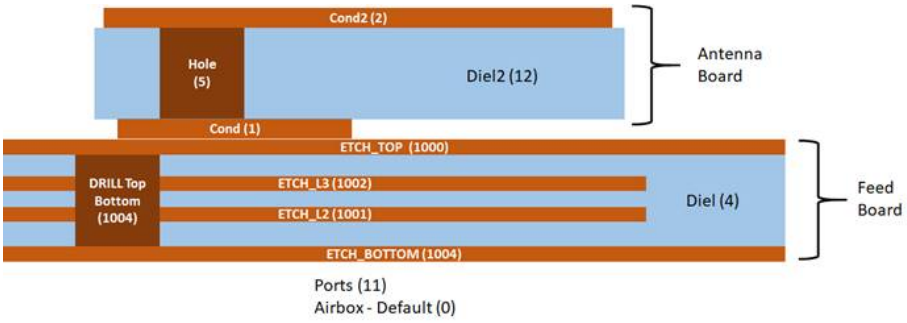

Figure 5.15: An overview of the new layering.

Chapter 6
Measurements Results

6.1 Prototype Results

In this chapter the results of the various simulations and measurements are presented. As this thesis goal is to find the smallest non compromised AoA implementable antenna array the results and our thought process behind going into further tests need to be discussed. This is presented in Chapter 8.

The results of the physical measurements ended up being 11 different large excel spreadsheets, where the angle estimation error, the measured angle and the average for the two are represented. This for 10 different measurements at each incoming angle for each different antenna element spacing. The bulk of the sheets are found in the Appendix A while a description of how they are to be interpreted is given in this section, as well as a representation of the result of highest interest for the purpose of thesis which is discussed in greater detail.

The top column represents the incoming angle from where the transmitter was placed. Below every angle of incidence the estimated angle is represented to the left and the deviation from the actual angle to the right under the title error see Figure 6.1. The following 10 rows under each incoming angle are the 10 different measurements taken at that specific angle see Figure 6.2. Lastly the final column is the average of the estimated angle and the estimation error for each incoming angle see Figure 6.3.

actual	10		20		30		40		
measured	angle	error	angle	error	angle	error	angle	error	an
	-90	10	-90	20	-65.2	5.2	-62.9	12.9	
	-90	10	-90	20	-64.4	4.4	-62.7	12.7	
	-90	10	-90	20	-64.5	4.5	-63.6	13.6	
	-90	10	-90	20	-68	8	-64.1	14.1	

Figure 6.1: The actual angle of incidence is given in the top row.

actual	10		
measured	angle	error	angle
	-90	10	-9
	-90	10	-9
	-90	10	-9
	-90	10	-9
	-90	10	-9
	-90	10	-9
	-90	10	-9
	-90	10	-9
	-90	10	-9
	-90	10	-9
Average	-90	10	-9

Figure 6.2: The result for each individual measurement.

	-90	10	-90	20	-64.9	4.9	-64.9
	-90	10	-90	20	-65.9	5.9	-63.8
Average	-90	10	-90	20	-65.64	5.64	-63.49

Figure 6.3: The average of the measurement.

Following this one can study the performance of each spacing, based on previous specification one can identify the smallest spacing that still meets the requirements. The specifications that we were assigned to were the maximum angle error of 10 degrees and a field of view at around 90 degrees. With this in mind we chose to go with the antenna element spacing of 0.3λ as the average angle error from 40 to 130 degrees were below 10 degrees, the spacing of 0.5λ performed better but since the goal of the thesis is to reduce the size, 0.3λ was chosen. The excel sheet for 0.3λ spacing is compiled in Table 6.1.

Incident angle	Average error
10	19.87
20	17.2
30	26.69
40	9.61
50	1.92
60	10
70	4.65
80	0.84
90	2.68
100	4.65
110	4.97
120	4.5
130	2.59
140	27.88
150	109.93
160	48.98
170	120.78

Table 6.1: Measurement results for 0.3λ.

These results were taken into account during the setup of the simulations.

Chapter 7
Simulation Results

7.1 Matlab Simulation

The Matlab simulation gave us results presented in the same fashion as the measurement results. The error that is presented is the average absolute error over 100 iterations. Every row represents the average error over those iterations for ascending antenna element spacings going in the negative y direction. The spacings range from 0.25λ to 0.5λ with an increase of 0.025λ spacing for each row. From the results it is noticeable that for spacings of 0.3λ and larger AoA is reasonably implementable. Although some spacings larger than 0.3λ performed better we found that 0.3λ acted as a limit for how small of a spacing is implementable without compromising performance that much.

The scalable parameters were set according to Table 7.1.

G_r	2 dB
G_t	2 dB
P_t	4 dBW
radius	4 m
noisefloor	-50 dBW

Table 7.1: Values of the scalable parameters in the Matlab script for signals strength and noise floor.

In Figure 7.1 and 7.2 the delimitations have been highlighted to show where in red the errors are consistently to large, which means that the field of view is limited to exclude these angles. In green is the error for 0.3λ spacing where that particular spacing starts to be of interest, since the physical measurements pointed to this specific spacing. In Appendix A the full spread sheet can be found and in Table 7.2 the errors for 0.3λ spacing is presented in intervals of 10 degrees. Analyzing Table A.3 in Appendix A the 0.3λ spacing can arguably be considered as the best candidate for further simulations in HFSS. Table A.4 in Appendix A shows the angle errors when the noise floor is at -40 dBW, here the errors are way

30	35	40	45	50	55
18.481	12.114	5.362	4.651	3.999	2.414
18.673	14.655	9.504	5.5	2.587	2.262
13.928	9.519	6.585	4.529	3.579	5.913
18.734	10.123	9.544	4.566	2.004	2.273
13.047	9.587	5.243	6.931	4.302	5.613
12.44	9.27	7.326	6.501	2.141	3.084
11.661	8.83	6.797	4.768	5.588	1.434
10.958	10.499	4.972	3.912	2.322	2.97
6.702	5.602	5.424	4.655	4.026	2.498
11.882	5.402	5.047	2.379	3.324	2.205
16.388	6.183	7.336	5.379	1.8	2.081

Figure 7.1: Cutout of the spreadsheet Matlab produced for 0.3λ spacing, angles 30 to 55.

120	125	130	135	140	145	150
2.643	3.314	4.596	5.724	9.52	6.701	12.987
1.679	5.356	3.28	6.777	7.135	10.654	14.486
2.326	3.85	6.123	7.744	5.575	10.325	15.565
3.791	1.709	3.229	8.071	6.707	9.527	11.431
1.467	6.639	6.012	4.108	5.227	9.941	12.763
1.65	3.509	4.708	5.158	6.58	7.979	9.474
1.832	4.599	4.039	4.045	8.327	8.113	9.809
2.831	2.718	3.861	6.811	4.533	11.644	14.998
4.296	3.532	4.022	4.439	3.834	7.638	13.733
1.201	1.681	2.06	4.542	4.069	4.477	13.433
2.394	3.406	3.859	2.121	6.634	13.135	14.912

Figure 7.2: Cutout of the spreadsheet Matlab produced for 0.3λ spacing, angles 120 to 150.

too large and therefore no conclusion could be made and on the other hand Table A.5 shows the errors when the noise floor is at -80 dBW and in this case there are no errors at all which also means that no conclusion could be made. Note that all these cases were simulated with the same parameters and the only altered one was the noise floor. This shows that the only thing that mattered is the SNR between the synthetically generated signal and the noise floor in these simulated measurements and is not the case in the real measurements. This means that we can only draw conclusions on which spacings perform well when the SNR is at a point where the algorithm performs similar to the physical measurements which in this case was when the noise floor was at -50 dBW.

Incident angle	Average error
10	69.15
20	28.90
30	13.93
40	6.59
50	3.58
60	2.09
70	2.44
80	1.19
90	1.72
100	1.23
110	1.25
120	2.33
130	6.12
140	5.58
150	15.57
160	29.03
170	60.67

Table 7.2: Simulation results for 0.3λ spacing.

7.2 HFSS

The following figures show the results of the first iteration of the shield before the layers were rearranged. The figures are the results from when port 1 in Figure 5.10 was excited. As seen in Figure 7.3 the excitation shows resonance at just below 2.44GHz. In Figure 7.4 we see that the impedance is 62-15j Ohms. In Figure 7.5 the radiation pattern is seen and shows great omnidirectional properties, Figure 7.6 shows the omnidirective properties for the excitation maximum elevation. Figure 7.7 show a 2D gain plot at 0 azimuth angle where the maximum gain is 2.55dB and the 3dB field of view is 99 degrees which we accept as being close enough to the previously set 100 degree requirement for the field of view.

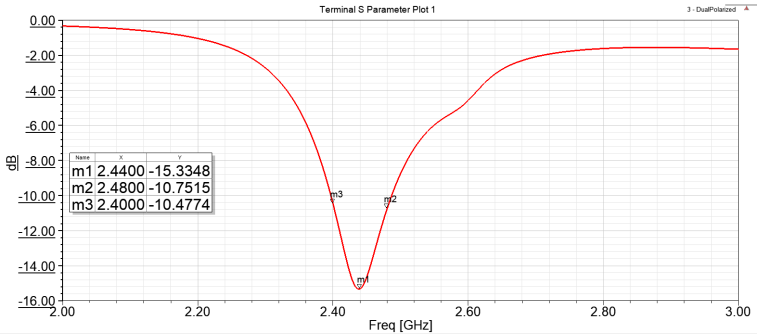

Figure 7.3: S11, simulation result for the first shield in HFSS.

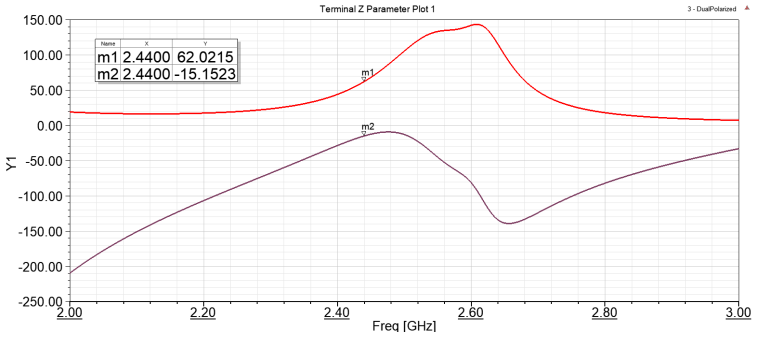

Figure 7.4: Impedance, simulation result for the first shield in HFSS. Red line is the real part and purple is the imaginary part.

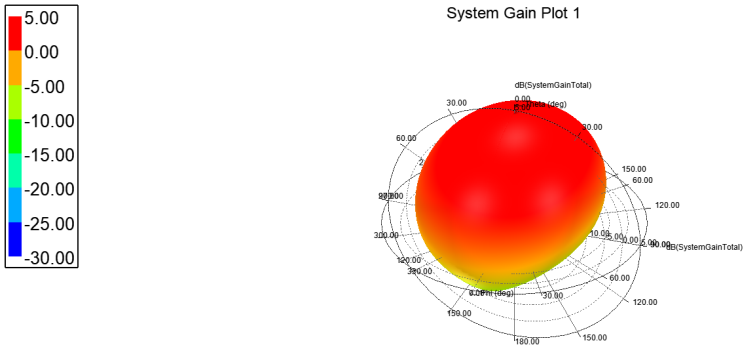

Figure 7.5: 3D Radiation Pattern, simulation result for the first shield in HFSS.

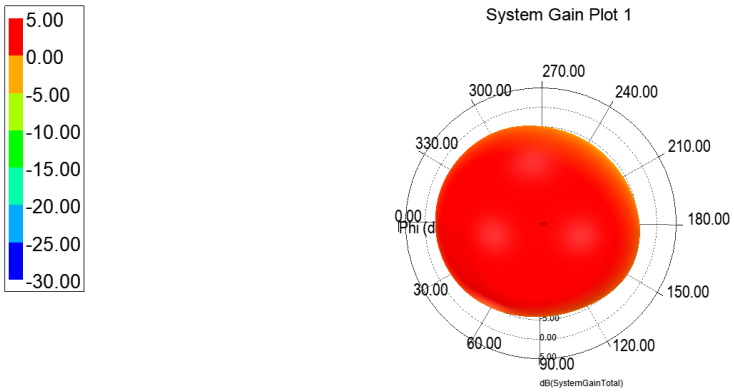

Figure 7.6: 3D Radiation Pattern, top side view, simulation result for the first shield in HFSS.

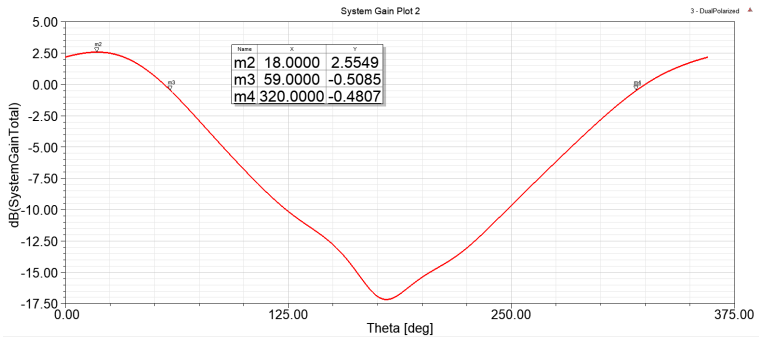

Figure 7.7: 2D Radiation Pattern,phi = 0, simulation result for the first shield in HFSS.

7.2.1 Altered layering

The following figures depict the results of the HFSS simulation once the layers had been altered to simulate the design which went into production. As can be seen in Figure 7.8 the resonance has been shifted into higher frequencies at around 2.55GHz, Figure 7.9 shows the new impedance plot. As seen in Figure 7.10 and Figure 7.11 the omnidirectionality is not compromised at all and the maximum new gain can be seen in Figure 7.12 which turned out to be around -0.09dB which is lower than an isotropic antenna. Note that this simulated value is with the whole system in mind where the excitation was put at the end of the transmission line feeding the antenna which means that losses in the transmission lines are taken into account. These new results is what can expected from the fabricated shield and was used to compare simulations to measurements.

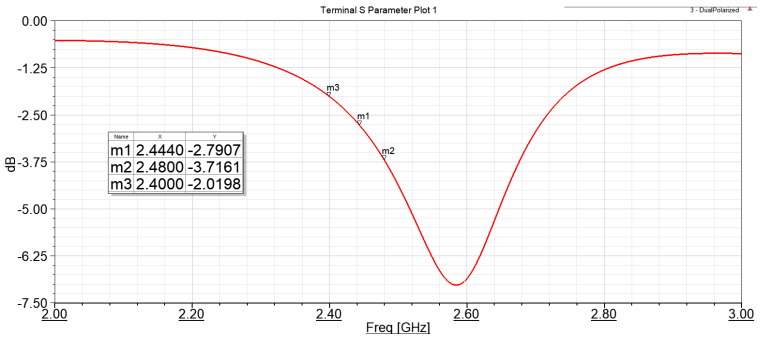

Figure 7.8: S11, simulation result for the second shield in HFSS.

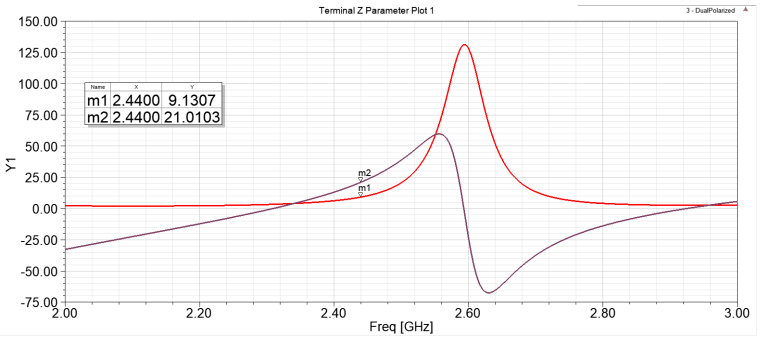

Figure 7.9: Impedance, simulation result for the second shield in HFSS.Red line is the real part and the purple line is the imaginary part.

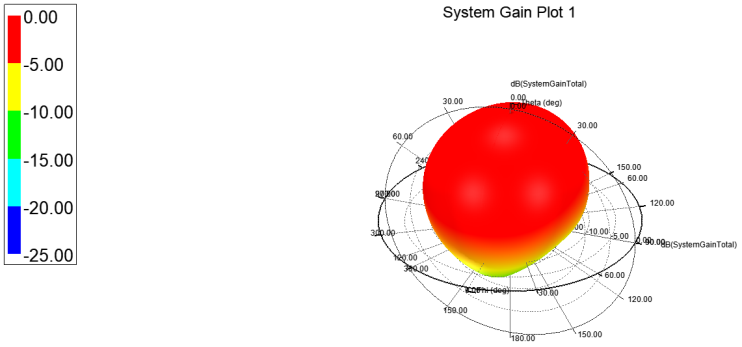

Figure 7.10: 3D Radiation Pattern, simulation result for the second shield in HFSS.

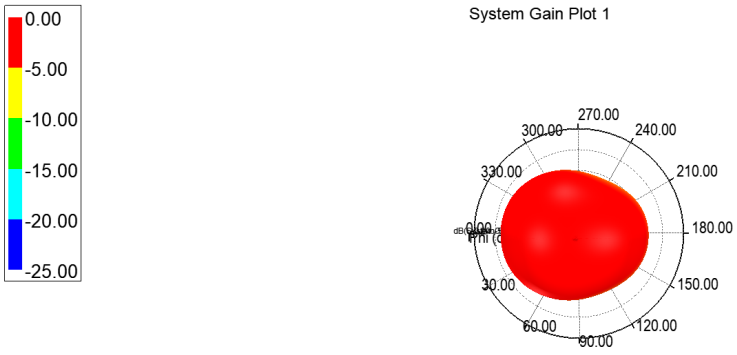

Figure 7.11: 3D Radiation Pattern, top side view, simulation result for the second shield in HFSS.

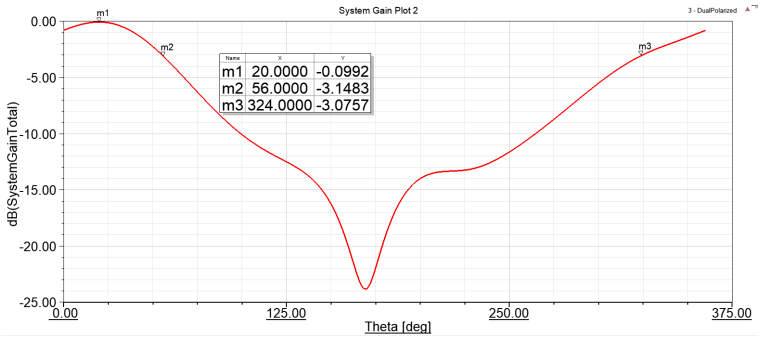

Figure 7.12: 2D Radiation Pattern,phi = 0, simulation result for the second shield in HFSS.

Chapter 8
Discussion

8.1 IQ-sampling

The reasoning behind our own matlab scripts for finding the angle of arrival of a set of IQ samples was to have full control over what values and what pairs behaved as they did. Instead of using already working programs that generates a random value, we on the other hand could figure out for example if the value was incorrect or what might have caused it to be so precise. A lot of time was spent early on in the thesis work to create these scripts. First we were to manually look at all the signals in time and with the help of markers distinguish the phase difference between antenna elements which in turn (with the spacing known) could give us the angle of arrival. This however turned out to be highly inconsistent as if there were to be a big deviation at the start or end of an IQ set of 16 pairs then it would be very difficult to find out about the true angle difference. This also turned out to be naive as we in this case only looked at the first IQ sample per antenna which is severely limiting the information from the total data. The code went through a lot of iterations and we finally ended up with a MUSIC algorithm which used all the data as well as estimating the angle of arrival for us. The MUSIC algorithm provided what could be seen as a bandwidth for the AoA measurements as the peak had different widths dependent on how noisy the signals were. This could be used to provide further information and intelligence to the algorithm but was not used in this thesis work as it did not seem necessary. All in all we were able to write scripts implementing a MUSIC algorithm where we can extract any value, IQ pair or angle of arrival to our liking which came in great help for understanding how faulty samples affects the measurements.

8.2 Physical measurement

There are two types of results, one that is corrected and one that is not altered at all. The issue is that sometimes the MUSIC algorithm would find two peaks and it only acknowledges the highest of the two peaks, it has no intelligence to distinguish which one of the two peaks is correct from past experiences. Therefore we acted as its intelligence and chose the correct peak manually and put it into the results. We also decided to correct the values if the error was very large at a certain angle and if the two angles surrounding it had very small errors. Theo-

retically there is no reason for the error to be so large at that specific angle and a second measurement was taken. Looking at the chosen spacing 0.3λ it can be argued that the reason for its values being better than the higher spacing was just luck, because the synthetic values showed a consistent loss in performance the smaller the spacing got and the physical measurements on the contrary did not. We tried to counteract this by taking 10 samples at each spacing and at each incident angle and make an average but seemingly that was not sufficient to mimic the behavior of the synthetic values. This raises the question if 0.3λ is the best contender for our work. The two smaller values 0.2 and 0.25λ both performed badly and a significant decrease in spacing was the goal therefore 0.3 was chosen otherwise we feel that the decrease in spacing would not be enough to warrant a new product. When the generated values were tested below 0.25λ all the way down to 0.1λ the angle error turned out to be way too large (with the same parameters 0.3λ performed well with) seen in Figure A.6 in Appendix A. This tells us that even in ideal situations smaller spacings than 0.25λ are irrelevant. This raises a second question is that a result of the actual spacing or this can be improved with a better MUSIC algorithm since the one used was rather simple with no intelligence. Also worth mentioning is the size of the antenna element acting as a lower bound of the possible spacings. For example if the antenna elements total length $= 0.25\lambda$ then it becomes impossible to have lower spacing than that in order to keep the elements separated which was sought after. A study that weighted the antenna size reduction versus reduced performance could be created in order to find a function that shows the least losses per reduced spacing, which can be done with the measured data. However since the resolution was 10 degrees it might not have been all that useful for the physical measurements. It could be done with the generated values as we choose the resolution. This however was not the goal of the thesis and was not done and therefore as stated earlier the smallest spacing that performed above the requirement was chosen.

Another aspect that might have impacted the physical measurements is that we took the ten measurements per angle and per spacing directly after each other which means that if there was some unforeseen impairing effect at that time that might have caused all the 10 samples to be affected the same way rendering the average tactic useless. If we could go back and do the measurements again we would have liked to not take the values after each other, and instead of setting a spacing and then going through all the angles with 10 samples each only doing 1 sample per angle and changing the spacing 10 times instead. This would be very time consuming but could improve the measurements. This seems to be the case since when some of the results turned out to be very bad a re-measurement was taken and that re-measurement always performed differently from the first one and usually better. However the main reason we did this in the first place was to not change the spacing at all for different incident angles, if we were to constantly change the spacing there is great inconsistency in accuracy since we changed spacing by hand. So rather than compromise the accuracy in spacing we compromised the accuracy in incident angle, but since the transmitter was not moved during the sampling time all samples had the same angle of incidence. The

angle might not have been exactly what was intended but all samples would be taken at the same angle which limits the room for errors and inconsistency. All in all we feel like the setup works and was able to measure AoA sufficiently and the main reason for even doing the physical measurements is to have something to compare with the generated values and try to find similarities in their behavior.

8.3 Synthetically generated data

It was quite difficult to mimic a noise floor in matlab as the theoretical noise floor in the script has nothing to do with an actual noise floor it is just supposed to have the same impact. Basically the theoretical noise floor is at the amplitude of the actual signals when the hardware starts to have issues finding the angle of arrival. It is at this point the results of the generated signals also start to have issues finding the angle of arrival as the signals used are as strong as the noise and therefore it becomes difficult for the algorithm to distinguish it and find a clear angle of arrival. However the physical measurements signals never appeared as noisy as the ones in the generated code but still the results were very similar and behaved roughly the same, as seen the physical signals were never low enough to encounter or be affected by the noise floor since they are not jagged like the noisy generated signals are. This was needed otherwise we would have to program the software used in the hardware inside the matlab code and that would mean creating an entire AoA system from scratch which is outside the scope of this thesis, so this shortcut was taken.

In the results of the matlab measurements the received power of the receiving antenna was calculated to be -44.36 dBW and the noise level was set to -50 dBW, which means that at an SNR of 5.64 the algorithm starts to produce large errors towards the outer edges of the angle spectrum. This resembles the behavior of the physical measurements. For these reasons we decided on these values for the scalable parameters as presented in 7.1. Note that the generated values could always be altered to give us good results but at the cost of being reasonable. If we lowered the noise floor too much the algorithm would always find the correct angle and would result in 0 errors due to the SNR being very large, likewise we could keep the noise floor high but increase the output power enough to get a good enough SNR to give the same results. Also it was quite difficult to find which SNR was needed in order to find a good trade off where the middle angles i.e 60-120 degrees performed well which they should most of the time but still see a significant decrease in performance on the outer angles. This was done manually, running the program with different SNRs until the results showed us what we wanted to see. This also means that all the SNRs above the one presented results in better AoA measurements than presented but in these cases we think it always better to find the limitations of the system rather than its possible performance.

8.4 Simulation results

Regarding the HFSS simulation of the shield, it produced good results with good resonance around the correct bluetooth frequency. It had low reflection at the specific frequency band and was omnidirectional as well as showing good peak gain of 2.55 dB.. The layering used was taken from an older schematic that was provided. These results and layout were sent to our company supervisor to be made ready for manufacturing. During this process the layering had to be changed in order to manufacture it due to various reasons which of course compromises the previous results. This in turn required new simulations with the altered layering, which results would be used as a guideline as to what could be expected from the measurements of the shield. This resulted in a shifted resonance frequency and much lower gain than originally expected from the first layering.

Chapter 9
Conclusion

A size reduced antenna was simulated and later put into manufacturing for later verification. The antenna array simulated with the original layering showed great resonance for BLE where the entire bluetooth frequency spectrum had S11 below -10dB, and a radiation pattern where the field of view is 99 degrees which is close enough to the previously set 100 degree specification with good peak gain. It is also sufficiently matched to 50 Ohms resulting in good reflection coefficient. With this in mind, the simulated antenna would perform better than the prototype originally used. The altered layered antenna that is in manufacturing is not guaranteed to perform as well as the simulated one, although the altered layered antenna is tunable and can be altered to achieve similar results as the original layered antenna.

The question regarding array size reduction is broad and the antenna spacing parameter has the largest impact on the total size. In this thesis the results point to that achieving AoA for antenna spacings smaller than 0.3λ tend to perform poorly compared with the typical value of 0.5λ. When the spacing decreases further below 0.25λ the possibility to achieve reliable AoA becomes increasingly more difficult. Having a complex AoA algorithm might enable one to decrease the spacing further than 0.25λ, but the inherited issues compact spacings cause will always be present.

To conclude a size reduced antenna array with antenna spacings of 0.3λ has been simulated showing great potential for use in BLE 5.1 for AoA.

Chapter 10
Future work

A second round of manufacturing the shield should be done due to the fact that the shield as of now is not tuned for its layer structure. So additional tuning in HFSS is needed before another shield can be produced. This to simply improve the performance of the product. A final test would also be desirable in a working environment with other bluetooth devices to see if the shield performers as intended in such an environment.

Regarding the size reduction, the total size can be made smaller if smaller antennas are used, this however needs to be looked into further. Since in this thesis spacing has been measured feed point to feed point a smaller antenna should not reduce the size drastically since the spacing is the main bottleneck in size reduction. Another aspect of using smaller antennas is that having three large antennas at a certain spacing and total array length does not imply better AoA capabilities than a greater number of smaller antennas with tighter spacing resulting in the same total array size. To improve upon this a study can be made studying the trade off between large mutual coupling between tightly spaced smaller antennas versus a larger amount of input data provided by the greater amount of antennas used. Another subject that is of interest is that making the antenna smaller would decrease mutual coupling, could this in turn be an argument for decreasing the spacing. Since a decrease in mutual coupling would increase performance, this implies that a smaller shield with smaller antennas could be made and perform equally as the shield in this paper. These subjects need further investigation which were beyond the scope of this thesis.

Improvements of Matlab algorithm could be made to resemble reality even more as to include radiation pattern and mutual coupling as well as making it more automated.

Appendix A

Appendix A

In this chapter images of how the incoming IQ-samples are depicted as an array and as a matrix. The array is what the input looked like once the I and Q values had been separated, the matrix is the whole input to the music algorithm. Although the whole matrix was not inserted at once, but every third column since that corresponds to a single antenna elements input. Following are the results from the MUSIC algorithm for various SNRs which are placed here for reference in regards to performance at different antenna spacings.

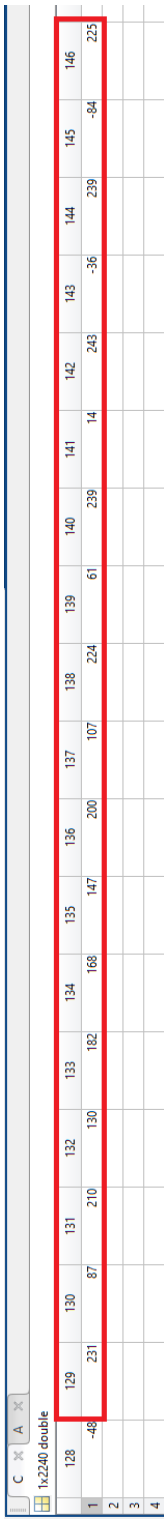

Figure A.1: Nine IQ samples in array format.

C A

32x33 complex double

	1	2	3
1	2.3100e+02 + 8.7000e+01i	2.2500e+02 ...	2.5500e+
2	2.1000e+02 + 1.3000e+02i	2.0900e+02 ...	2.5400e+
3	1.8200e+02 + 1.6800e+02i	1.9100e+02 ...	2.5000e+
4	1.4700e+02 + 2.0000e+02i	1.7100e+02 ...	2.4900e+
5	1.0700e+02 + 2.2400e+02i	1.4700e+02 ...	2.5500e+
6	6.1000e+01 + 2.3900e+02i	1.2000e+02 ...	2.6700e+
7	1.4000e+01 + 2.4300e+02i	8.6000e+01 ...	2.8700e+
8	-3.6000e+01 + 2.3900e+02i	4.6000e+01 ...	3.1200e+
9	-8.4000e+01 + 2.2500e+02i	2.0000e+00 ...	3.3600e+
10	-1.2800e+02 + 2.0000e+02i	-4.5000e+0...	3.5700e+
11	-1.6800e+02 + 1.6600e+02i	-9.3000e+0...	3.6800e+
12	-2.0000e+02 + 1.2700e+02i	-1.3900e+0...	3.6400e+
13	-2.2400e+02 + 8.0000e+01i	-1.7900e+0...	3.4400e+
14	-2.3800e+02 + 3.1000e+01i	-2.1000e+0...	3.0800e+
15	-2.4200e+02 - 1.9000e+01i	-2.3100e+0...	2.5600e+
16	-2.3600e+02 - 6.6000e+01i	-2.4100e+0...	1.9200e+
17	-2.2200e+02 - 1.1100e+02i	-2.4000e+0...	1.2300e+
18	-1.9800e+02 - 1.5000e+02i	-2.3000e+0...	4.9000e+
19	-1.6500e+02 - 1.8300e+02i	-2.1100e+0...	-2.3000e
20	-1.2600e+02 - 2.0900e+02i	-1.8300e+0...	-9.3000e
21	-8.1000e+01 - 2.2700e+02i	-1.5100e+0...	-1.5700e
22	-3.2000e+01 - 2.3600e+02i	-1.1200e+0...	-2.1500e
23	1.7000e+01 - 2.3600e+02i	-6.8000e+0...	-2.6500e
24	6.7000e+01 - 2.2800e+02i	-2.0000e+0...	-3.0500e
25	1.1300e+02 - 2.0900e+02i	2.7000e+01 ...	-3.3200e
26	1.5600e+02 - 1.8300e+02i	7.4000e+01 ...	-3.4600e
27	1.9100e+02 - 1.5000e+02i	1.1900e+02 ...	-3.4400e
28	2.1900e+02 - 1.1100e+02i	1.5900e+02 ...	-3.2900e
29	2.3800e+02 - 7.0000e+01i	1.9200e+02 ...	-3.0300e
30	2.4700e+02 - 2.9000e+01i	2.1900e+02 ...	-2.7300e
31	2.4600e+02 + 1.0000e+01i	2.3800e+02 ...	-2.4300e
32	2.3800e+02 + 4.4000e+01i	2.5100e+02 ...	-2.1600e

Figure A.2: Nine IQ samples in matrix format.

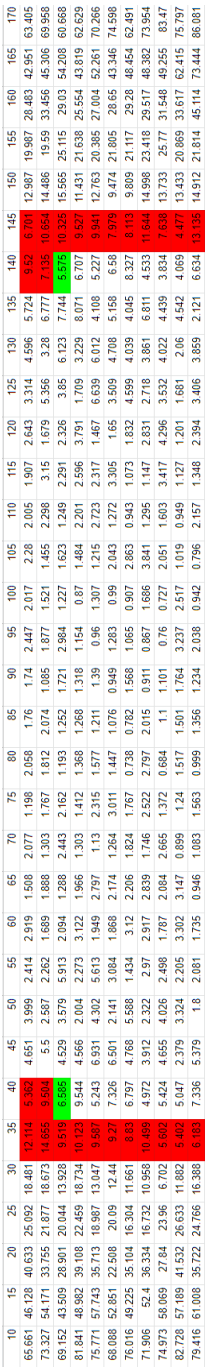

10	15	20	25	30	35	40	45	50	55	60	65	70	75	80	85	90	95	100	105	110	115	120	125	130	135	140	145	150	155	160	165	170
65.661	46.128	40.633	25.092	18.481	12.114	5.362	4.651	3.999	2.414	2.919	1.508	2.077	1.198	2.058	1.76	1.74	2.447	2.017	2.28	2.005	1.907	2.643	3.314	4.596	5.724	9.52	6.701	12.987	19.987	28.483	42.951	63.405
73.327	54.171	33.755	21.877	18.673	14.655	9.504	5.5	2.587	2.262	1.689	1.888	1.303	1.767	1.812	2.074	1.085	1.877	1.521	1.455	2.298	3.15	1.679	5.356	3.28	6.777	7.135	10.654	14.486	19.59	33.456	45.306	69.958
69.152	43.509	28.901	20.044	13.928	9.519	6.556	4.529	3.579	5.913	2.094	1.288	2.443	2.162	1.193	1.252	1.721	2.984	1.227	1.623	1.249	2.291	2.326	3.85	6.123	7.744	5.575	10.325	15.565	25.115	29.03	54.208	60.668
81.841	48.982	39.108	22.459	18.734	10.123	9.544	4.566	2.004	2.273	3.122	1.966	1.303	1.412	1.368	1.268	1.318	1.154	0.87	1.484	2.201	2.596	3.791	1.709	3.229	8.071	6.707	9.527	11.431	21.638	25.554	43.819	62.629
75.771	57.743	35.713	18.987	13.047	9.587	5.243	6.931	4.302	5.613	1.949	2.797	1.13	2.315	1.577	1.211	1.39	0.96	1.307	1.215	2.723	2.317	1.467	6.639	6.012	4.108	5.227	9.941	12.763	20.385	27.004	52.261	70.266
68.088	52.851	22.508	20.09	12.44	9.27	7.326	6.501	2.141	3.084	1.868	2.174	1.264	3.011	1.447	1.076	0.949	1.283	0.99	2.043	1.272	3.305	1.65	3.509	4.708	5.158	6.58	7.979	9.474	21.805	28.65	43.346	74.598
76.016	49.225	35.104	16.304	11.661	8.83	6.797	4.768	5.588	1.434	3.12	2.206	1.824	1.767	0.738	0.782	1.568	1.065	0.907	2.863	0.943	1.073	1.832	4.599	4.039	4.045	8.327	8.113	9.809	21.117	29.28	48.454	62.491
71.906	52.4	36.334	16.732	10.958	10.459	4.972	3.912	2.322	2.97	2.917	2.839	1.746	2.522	2.797	2.015	0.911	0.867	1.686	3.841	1.295	1.147	2.831	2.718	3.861	6.811	4.533	11.644	14.998	23.418	29.517	48.382	73.954
74.973	58.069	27.84	23.96	6.702	5.602	5.424	4.655	4.026	2.498	1.787	2.084	2.665	1.372	0.684	1.1	1.101	0.76	0.727	2.051	1.603	3.417	4.296	3.532	4.022	4.439	3.834	7.638	13.733	25.77	31.548	49.255	83.47
82.728	57.189	41.532	26.633	11.882	5.402	5.047	2.379	3.324	2.205	3.302	3.147	0.899	1.24	1.517	1.501	1.764	3.237	2.517	1.019	0.949	1.127	1.201	1.681	2.06	4.542	4.069	4.477	13.433	20.869	33.617	62.415	75.797
79.416	61.008	35.722	24.766	16.388	6.163	7.336	5.379	1.8	2.081	1.735	0.946	1.083	1.563	0.999	1.356	1.234	2.038	0.942	0.796	2.157	1.348	2.394	3.406	3.859	2.121	6.634	13.135	14.912	21.814	45.114	73.444	86.081

Figure A.3: Matlab simulation results -50dBW noise floor.

	0.25λ	0.275λ	0.3λ	0.325λ	0.35λ	0.375λ	0.4λ	0.425λ	0.45λ	0.475λ	0.5λ
170	68	82	91	82	84	92	86	83	84	76	82
165	86	71	80	78	77	74	78	75	76	76	76
160	75	81	71	86	73	81	79	73	72	72	67
155	64	74	69	62	71	62	65	62	62	68	64
150	60	65	65	62	52	62	55	56	57	62	60
145	50	56	65	55	62	51	49	58	49	53	52
140	53	54	57	57	46	43	45	45	47	43	40
135	44	37	43	55	38	41	46	33	41	38	39
130	34	47	40	34	32	38	35	35	27	27	29
125	36	38	35	25	41	30	22	27	26	24	30
120	32	28	22	34	24	25	24	24	20	24	25
115	23	30	28	32	30	21	18	23	23	20	18
110	22	23	26	27	19	20	25	20	23	17	15
105	16	25	18	19	26	22	25	18	19	15	18
100	15	18	17	16	20	18	16	17	16	16	15
95	19	17	18	14	23	20	23	19	17	17	11
90	16	19	17	21	14	18	13	15	15	14	14
85	22	15	20	18	20	19	16	22	14	18	13
80	21	20	19	17	19	20	26	18	18	14	18
75	18	21	18	22	22	26	17	19	18	16	13
70	22	23	25	21	28	18	19	21	19	16	19
65	26	18	23	25	27	20	30	22	19	18	22
60	29	30	29	26	27	27	27	20	21	24	20
55	31	35	37	32	36	26	31	25	24	25	25
50	38	39	40	40	41	30	41	33	30	31	25
45	41	41	41	45	41	44	39	37	36	39	32
40	56	52	49	54	50	46	50	42	45	42	47
35	53	58	56	50	62	54	48	51	49	42	47
30	60	61	67	59	61	57	61	65	61	60	57
25	65	71	80	73	67	73	70	69	63	61	64
20	72	77	84	63	79	76	78	71	68	68	69
15	84	72	80	85	72	80	77	69	76	78	78
10	90	92	90	79	71	81	84	81	82	76	79

Figure A.4: -40dB noise, very large errors.

	0.25λ	0.275λ	0.3λ	0.325λ	0.35λ	0.375λ	0.4λ	0.425λ	0.45λ	0.475λ	0.5λ
170	1	0	0	0	0	0	0	0	0	0	1
165	0	0	0	0	0	0	0	0	0	0	0
160	0	0	0	0	0	0	0	0	0	0	0
155	0	0	0	0	0	0	0	0	0	0	0
150	0	0	0	0	0	0	0	0	0	0	0
145	0	0	0	0	0	0	0	0	0	0	0
140	0	0	0	0	0	0	0	0	0	0	0
135	0	0	0	0	0	0	0	0	0	0	0
130	0	0	0	0	0	0	0	0	0	0	0
125	0	0	0	0	0	0	0	0	0	0	0
120	0	0	0	0	0	0	0	0	0	0	0
115	0	0	0	0	0	0	0	0	0	0	0
110	0	0	0	0	0	0	0	0	0	0	0
105	0	0	0	0	0	0	0	0	0	0	0
100	0	0	0	0	0	0	0	0	0	0	0
95	0	0	0	0	0	0	0	0	0	0	0
90	0	0	0	0	0	0	0	0	0	0	0
85	0	0	0	0	0	0	0	0	0	0	0
80	0	0	0	0	0	0	0	0	0	0	0
75	0	0	0	0	0	0	0	0	0	0	0
70	0	0	0	0	0	0	0	0	0	0	0
65	0	0	0	0	0	0	0	0	0	0	0
60	0	0	0	0	0	0	0	0	0	0	0
55	0	0	0	0	0	0	0	0	0	0	0
50	0	0	0	0	0	0	0	0	0	0	0
45	0	0	0	0	0	0	0	0	0	0	0
40	0	0	0	0	0	0	0	0	0	0	0
35	0	0	0	0	0	0	0	0	0	0	0
30	0	0	0	0	0	0	0	0	0	0	0
25	0	0	0	0	0	0	0	0	0	0	0
20	0	0	0	0	0	0	0	0	0	0	0
15	0	0	0	0	0	0	0	0	0	0	0
10	0	0	0	0	0	0	0	0	0	0	0

Figure A.5: -80dB noise, very low errors.

	0.1λ	0.14λ	0.18λ	0.22λ	0.26λ	0.30λ	0.34λ	0.38λ	0.42λ	0.46λ	0.5λ
170	83	82	72	93	78	84	81	83	90	86	80
165	100	81	71	87	95	81	71	84	72	76	76
160	71	70	64	69	65	79	72	69	76	69	73
155	72	65	65	60	67	65	63	58	56	63	71
150	55	58	50	53	46	45	47	43	54	51	51
145	45	37	42	35	41	41	34	31	34	34	37
140	37	33	25	24	28	23	28	21	17	20	21
135	32	25	19	22	14	15	20	11	11	12	8
130	25	18	16	12	9	7	11	7	8	6	6
125	21	15	12	7	7	7	6	5	4	4	4
120	19	11	9	8	6	5	4	4	4	3	3
115	12	9	8	6	5	4	3	4	3	2	2
110	12	9	6	5	4	4	3	3	3	2	2
105	11	7	5	5	3	4	3	3	2	2	2
100	9	5	5	4	4	3	3	2	2	2	2
95	9	7	5	4	3	3	3	2	2	2	2
90	10	6	6	4	4	3	3	3	2	2	2
85	9	6	5	4	4	3	2	2	2	2	2
80	10	7	6	4	4	3	3	2	3	2	2
75	10	8	6	4	4	3	3	2	2	2	2
70	11	7	6	5	5	4	3	3	3	2	2
65	14	8	6	6	4	4	4	3	3	3	2
60	14	10	9	7	6	5	4	4	4	3	3
55	22	13	11	7	6	6	6	5	5	4	3
50	23	17	16	12	9	8	8	7	6	6	5
45	28	24	17	21	21	14	9	11	13	9	8
40	36	29	29	33	27	23	28	21	23	18	18
35	51	41	39	38	36	36	35	38	36	43	31
30	51	56	44	53	52	55	49	56	45	48	52
25	70	57	67	67	58	62	63	57	62	65	60
20	72	79	67	71	74	77	67	66	68	76	73
15	79	81	80	81	86	85	77	67	84	80	73
10	77	82	95	90	89	85	86	78	86	77	79

Figure A.6: -50dB noise, very large errors for small spacings

References

[1] "Radar," The Free Dictionary. [Online]. Available: https://acronyms.thefreedictionary.com/RADAR

[2] C. Balanis, *Antenna theory-Analysis and Design. 3rd edition.* A John Wiley Sons, 2005, ch. 2,4, pp.33-35, 184-185. [Online]. Available: https://www.academia.edu/11205305/Antenna_Theory_Analysis_and_Design_3rd_Edition_by_Balanis

[3] "Dipole antenna radiation pattern," WOLFRAM Demonstrations Project, 2020. [Online]. Available: https://demonstrations.wolfram.com/DipoleAntennaRadiationPattern/

[4] "Introduction to rf & wireless communications systems," NI, 2020. [Online]. Available: http://www.ni.com/tutorial/3541/en/

[5] "Understanding bluetooth range," Bluetooth, 2020. [Online]. Available: https://www.bluetooth.com/learn-about-bluetooth/bluetooth-technology/range/

[6] *From cable replacement to the IoT Bluetooth 5.1*, Rohde & Schwarz, 2020. [Online]. Available: https://scdn.rohde-schwarz.com/ur/pws/dl_downloads/dl_application/application_notes/1ma108/1MA108_4e_Bluetooth_WhitePaper.pdf

[7] M. Cominelli, P. Patras, and F. Gringoli, "Dead on arrival: An empirical study of the bluetooth 5.1 positioning system," in *Proceedings of the 13th International Workshop on Wireless Network Testbeds, Experimental Evaluation & Characterization*, 2019, pp. 13–20.

[8] D. Porter and R. Myhr, *Bluetooth® Angle of Arrival (AoA) Antenna Design*, Texas Instruments, 2020. [Online]. Available: http://www.ti.com/lit/an/tida029/tida029.pdf?ts=1590742257648

[9] P. Baltrenas, R. Buckus, and V. Saulius, "Research and evaluation of the intensity parameters of electromagnetic fields produced by mobile communication antennas," *Journal of Environmental Engineering and Landscape Management*, vol. 20, pp. 273–284, 11 2012.

[10] S. J. Orfanidis, "Electromagnetic waves and antennas," 2002. [Online]. Available: https://www.ece.rutgers.edu/~orfanidi/ewa/

[11] H. L.Sundström, G.Jönsson, *Radio Electronics*. Lund University, 2015, ch. 3.

[12] Antenna-theory, "Microstrip (patch) antennas," Online, 2016. [Online]. Available: http://www.antenna-theory.com/antennas/patches/antenna.php

[13] H. Werfelli, K. Tayari, M. Chaoui, M. Lahiani, and H. Ghariani, "Design of rectangular microstrip patch antenna," in *2016 2nd International Conference on Advanced Technologies for Signal and Image Processing (ATSIP)*. IEEE, 2016, pp. 798–803.

[14] A. Alomainy, R. Di Bari, Q. H. Abbasi, and Y. Chen, *Co-operative and energy efficient body area and wireless sensor networks for healthcare applications*. Academic Press, 2014. [Online]. Available: https://www.sciencedirect.com/topics/engineering/antenna-performance

[15] J. R. Pereira and P. Pinho, "Using the Smith chart in an e-learning approach," *Edited by Elvis Pontes, Anderson Silva*, p. 99, 2012. [Online]. Available: https://www.researchgate.net/publication/221925022_Using_the_Smith_Chart_in_an_E-Learning_Approach

[16] H. Singh, H. Sneha, and R. Jha, "Mutual coupling in phased arrays: A review," *International Journal of Antennas and Propagation*, vol. 2013, 2013. [Online]. Available: https://www.hindawi.com/journals/ijap/2013/348123/

[17] K. Buell, H. Mosallaei, and K. Sarabandi, "Metamaterial insulator enabled superdirective array," *IEEE Transactions on Antennas and Propagation*, vol. 55, no. 4, pp. 1074–1085, 2007.

[18] Fan Yang and Y. Rahmat-Samii, "Microstrip antennas integrated with electromagnetic band-gap (ebg) structures: a low mutual coupling design for array applications," *IEEE Transactions on Antennas and Propagation*, vol. 51, no. 10, pp. 2936–2946, 2003.

[19] "Rayleigh fading," Wireless Communication, 2020. [Online]. Available: http://www.wirelesscommunication.nl/reference/chaptr03/rayleigh.htm

[20] A. Bensky, *Short-range Wireless Communication*. Elsevier Science, 2019, ch. 2, p. 25. [Online]. Available: https://books.google.se/books?id=TtCmDwAAQBAJ

[21] P. Gupta and S. P. Kar, "Music and improved music algorithm to estimate direction of arrival," in *2015 International Conference on Communications and Signal Processing (ICCSP)*, 2015, pp. 0757–0761.

[22] M. Mohanna, M. L. Rabeh, E. M. Zieur, and S. Hekala, "Optimization of music algorithm for angle of arrival estimation in wireless communications," *NRIAG journal of Astronomy and Geophysics*, vol. 2, no. 1, pp. 116–124, 2013. [Online]. Available: https://www.sciencedirect.com/science/article/pii/S209099771300031X

[23] Nordic-Semiconductors, "nrf52 dk," Online, 2020. [Online]. Available: https://www.nordicsemi.com/Software-and-Tools/Development-Kits/nRF52-DK

[24] SEGGER, “Software tools for embedded systems,” Online, 2020. [Online]. Available: https://www.segger.com/products/software-development-tools/

[25] PuTTY, Online, 2020. [Online]. Available: https://www.putty.org/

[26] Matlab, Online, 2020. [Online]. Available: https://se.mathworks.com/products/matlab.html

[27] Ansys, Online, 2020. [Online]. Available: https://www.ansys.com/products/electronics/ansys-hfss/ansys-electronic-desktop

Printed by Tryckeriet i E-huset, Lund 2020

LUND
UNIVERSITY

Series of Master's theses
Department of Electrical and Information Technology
LU/LTH-EIT 2020-794
http://www.eit.lth.se